Journal of Quantitative Spectroscopy & Radiative Transfer 276 (2021) 107896

Contents lists available at ScienceDirect

Journal of Quantitative Spectroscopy & Radiative Transfer

journal homepage: www.elsevier.com/locate/jqsrt

# The update of the line positions and intensities in the line list of carbon dioxide for the HITRAN2020 spectroscopic database

E.V. Karlovets[a,b,*], I.E. Gordon[a,*], L.S. Rothman[a], R. Hashemi[a], R.J. Hargreaves[a], G.C. Toon[c], A. Campargue[d], V.I. Perevalov[e], P. Čermák[f], M. Birk[g], G. Wagner[g], J.T. Hodges[h], J. Tennyson[i], S.N. Yurchenko[i]

[a] Harvard-Smithsonian Center for Astrophysics, Atomic and Molecular Physics Division, 60 Garden St, Cambridge, MA, United States
[b] Tomsk State University, Laboratory of Quantum Mechanics of Molecules and Radiative Processes, 36, Lenin Avenue, 634050 Tomsk, Russian Federation
[c] Jet Propulsion Laboratory, California Institute of Technology, Pasadena, CA, United States
[d] University of Grenoble Alpes, CNRS UMR 5588, LIPhy, Grenoble F-38000, France
[e] V.E. Zuev Institute of Atmospheric Optics, 1, Academician Zuev square, 634055 Tomsk, Russian Federation
[f] Department of Experimental Physics, Faculty of Mathematics, Physics and Informatics, Comenius University, Mlynská dolina 842 48 Bratislava, Slovakia
[g] Remote Sensing Technology Institute, German Aerospace Center (DLR), D-82234 Wessling, Germany
[h] National Institute of Standards and Technology, Gaithersburg, MD 20899, United States
[i] Department of Physics and Astronomy, University College London, Gower Street, WC1E 6BT London, United Kingdom

ARTICLE INFO

*Article history:*
Received 20 May 2021
Revised 21 August 2021
Accepted 22 August 2021
Available online 25 August 2021

*Keywords:*
Carbon dioxide
$CO_2$ line lists
HITRAN2020
Spectroscopic line parameters

ABSTRACT

This paper describes the updates of the line positions and intensities for the carbon dioxide transitions in the 2020 edition of the HITRAN spectroscopic database. The new line list for all 12 naturally abundant isotopologues of carbon dioxide replaces the previous one from the HITRAN2016 edition. This update is primarily motivated by several issues related to deficient HITRAN2016 line positions and intensities that have been identified from laboratory and atmospheric spectra. Critical validation tests for the spectroscopic data were carried out to find problems caused by inaccuracies in $CO_2$ line parameters. New sources of data were selected for the bands that were deemed problematic in the HITRAN2016 edition. Extra care was taken to retain the consistency in the data sources within the bands. The comparisons with the existing theoretical and semi-empirical databases (including ExoMol, NASA Ames, and CDSD-296) and with available experimental works were carried out. The HITRAN2020 database has been extended by including additional $CO_2$ bands above 8000 $cm^{-1}$, and magnetic dipole lines of $CO_2$ were introduced in HITRAN for the first time by including the $\nu_2+\nu_3$ band in the 3.3-μm region. Although the main topic of this article is line positions and intensities, for consistency a recent algorithm for the line-shape parameters proposed in Hashemi et al. JQSRT (2020) was reapplied (after minor revisions) to the line list.


## 1. Introduction

A plethora of critical applications drives a constant demand for ever higher-quality spectroscopic parameters of carbon dioxide ($CO_2$) transitions. Atmospheric $CO_2$ is the key gaseous contributor to the greenhouse effect in the terrestrial atmosphere. Its continuous increase in the atmosphere over the last two centuries from anthropogenic sources is considered the principal driver of climate change. The Martian and Venusian (and those of many rocky exoplanets) atmospheres consist mostly of carbon dioxide with mole fractions of over 95%. Monitoring $CO_2$ is important in combustion. There are several satellite-based observatories, including GOSAT [1–3], GOSAT-2 [4], OCO-2 [5,6], OCO-3 [7], MIPAS [8], and ACE [9], as well as ground-based networks TCCON [10] and NDACC [11], monitoring atmospheric $CO_2$. Accurate interpretation of the data from these missions is necessary to make informed decisions regarding controlling the anthropogenic contribution to the greenhouse effect and, ultimately, climate change. All aforementioned $CO_2$ remote sensing activities depend on the reliability of the reference $CO_2$ spectroscopy.

The HITRAN molecular spectroscopic database is the widely recognized standard providing the spectroscopic data for atmospheric applications. Among many other molecules, it includes the necessary calculated and experimental parameters for all naturally abundant isotopologues of carbon dioxide. The HITRAN2016 [12] $CO_2$ line list for 12 stable isotopologues contains 559,874 transitions.

* Corresponding authors.
*E-mail addresses:* ekarlovets@gmail.com (E.V. Karlovets), igordon@cfa.harvard.edu (I.E. Gordon).

https://doi.org/10.1016/j.jqsrt.2021.107896
0022-4073/

Most of the issues related to spectral completeness (at least below 8000 $cm^{-1}$) and insufficient accuracy of line parameters were resolved in HITRAN2016 [12]. However, there is still a lot of room for improvement to meet the ever-increasing demands of the scientific community. Since the release of the HITRAN2016 database [12], many new experimental and theoretical data have become available, and they can be used as sources for improving line positions, line intensities, and line-shape parameters of $CO_2$. The HITRAN-related updates, including the $CO_2$-air and $CO_2$–$CO_2$ line-shape parameters together with the speed dependence of the broadening parameters, their temperature-dependent exponents, the full and first-order line mixing, as well as their temperature dependencies have been published in Hashemi et al. [13].

In the present work, we will mainly focus on the issues associated with deficiencies in the HITRAN2016 line positions and intensities. Most of these problematic cases have been identified in laboratory and atmospheric spectra, mainly from the Kitt Peak National Observatory, MkIV balloon, cavity ring down spectroscopy (CRDS) measurements, and the Total Carbon Column Observing Network (TCCON) [14–16]. A general review of the $CO_2$ bands affected by these issues was performed, and alternative sources of data for each $CO_2$ problematic band were considered. Apart from new experimental data, the additional resources for improvements were provided by two recent comprehensive $CO_2$ line lists, namely the 2019 version of the semi-empirical CDSD-296 [17] list and the ExoMol variational line list [18], hereafter referred to as UCL-4000. Using these spectroscopic data, we improved and extended the $CO_2$ line lists for all 12 stable isotopologues of carbon dioxide.

The updates of the line positions, intensities, and line-shape parameters were incorporated into the carbon dioxide line list of the 2020 edition of the HITRAN spectroscopic database. The remainder of this paper is organized as follows. In Section 2, we present an overview of $CO_2$ line lists in the HITRAN2016, ExoMol, NASA Ames, and CDSD-296 spectroscopic databases. In Section 3, we describe evaluations of the HITRAN $CO_2$ line list based on laboratory and atmospheric measurements between 670 and 8310 $cm^{-1}$. For wavenumbers below 8000 $cm^{-1}$, we discuss line intensity updates to the HITRAN2016 line list for bands provided by the Carbon Dioxide Spectroscopic Databank (CDSD) based on global fits of semi-empirical models to measurements and those obtained by the *ab initio* calculations of University College London (UCL). In Section 4, we discuss new measurements with sub-percent relative uncertainty [19–22] that were used to improve some $CO_2$ bands in the 1.4- to 2.1-μm region. In Section 5, we present new $CO_2$ bands above 8000 $cm^{-1}$ that have been included in the HITRAN2020 edition from the latest high-temperature line list of the ExoMol [18] database (with appropriate cut-off) for the main $CO_2$ isotopologue and the CRDS spectra [14] for the $^{16}O^{12}C^{18}O$ isotopologue. The line parameters of the $\nu_2+\nu_3$ magnetic dipole band of the $^{12}C^{16}O_2$ isotopologue, which have been introduced into HITRAN for the first time, will be presented in Section 6. The revision, which updates the air- and self-broadened line-shape parameters of $CO_2$, described in Ref. [13], will be discussed in Section 7. The presentation of the final version of the HITRAN2020 $CO_2$ line list will be given in Section 8, followed by a closing discussion and conclusions in Section 9.

## 2. Review of the current carbon dioxide line lists

The present section describes the status of the most currently used spectroscopic databases of carbon dioxide: HITRAN2016 [12], NASA Ames [23], and the recent ExoMol [18] and CDSD-296 [17] line lists. The laboratory and atmospheric spectra helped to expose several problems in the HITRAN2016 $CO_2$ line list occurring in various spectral regions (for more details, see Section 3). The CDSD-296, ExoMol, and NASA Ames line lists were used to update, extend or improve the line positions and intensities, including a number of problematic bands, resulting in the 2020 version of the HITRAN spectroscopic database [24].

The $CO_2$ line list for the 12 stable isotopologues in the 2016 version of HITRAN [12] contained 559,874 $CO_2$ transitions and covered the wavenumber range of 0.757–14,075.298 $cm^{-1}$. The HITRAN2016 data for the $^{14}C^{16}O_2$ radioactive isotopologue were provided as static files rather than through the relational database structure featured in HITRAN*online* [25]. The HITRAN2016 carbon dioxide line list, below 8000 $cm^{-1}$, comprised CDSD line positions [26] and *ab initio* line intensities from UCL [27–29] except for the bands that were identified as "sensitive" [27], where CDSD (circa 2015) intensity values were preferred. Most of the line parameters above 8000 $cm^{-1}$ were taken from the 2015 version of the CDSD-296 database [26]. An extended and improved version of the CDSD for atmospheric applications (CDSD-296) was published in 2019 [17]. This database contains a computed line list based on global modeling of the line positions and intensities using the method of effective operators [30,31]. The global model of the $CO_2$ absorption spectrum is a polyad model with a block diagonal structure, each polyad being characterized by the polyad number $P = 2V_1 + V_2 + 3V_3$ (where $V_i$ are the vibrational quantum numbers). For each $CO_2$ isotopologue, the effective Hamiltonians and effective dipole moment parameters were fitted to measured line positions and intensities, respectively. More than 530,000 spectral lines for the 12 stable isotopologues of $CO_2$ covering the 345–14,075 $cm^{-1}$ spectral range were included in this database. The reference temperature is 296 K, and the intensity cut-off is $10^{-30}$ cm/molecule. A comparison between the line positions of common lines from the HITRAN2016 and CDSD-296 [17] databases versus wavenumber in the 0–14,075 $cm^{-1}$ spectral region is presented in Fig. 1. This plot shows the good agreement between the line positions from HITRAN2016 (mostly based on the previous CDSD version [26]) and those from the new version of the CDSD-296 [17]. As a result, most of the line positions for the 12 $CO_2$ isotopologues between 345 and 14,075 $cm^{-1}$ in HITRAN2020, have been updated using the CDSD-296 [17] values. It should be noted that the slightly updated version of the CDSD-296 database (uploaded at ftp.iao.ru as pub/CDSD-296/cdsd-296_version_1.rar) was used. This version differs from the CDSD-296 published in Tashkun et al. [17] in the following ways: (*i*) the $\Delta P = 6$ region of the $^{16}O^{12}C^{18}O$ isotopologue was recalculated using the new set of effective dipole moment pa-

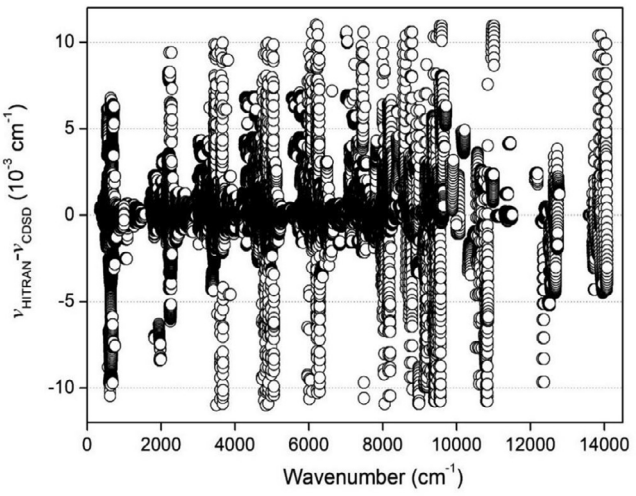


**Fig. 1.** Differences between the line positions from the HITRAN2016 [12] and CDSD-296 [17] databases.

rameters; (*ii*) a total of 226 lines with vibrational quantum number $\Delta l_2 = 4$ of the $^{12}C^{16}O_2$, $^{13}C^{16}O_2$, and $^{16}O^{12}C^{18}O$ isotopologues were added. The lower-state energies and the uncertainty codes were also transferred from the CDSD-296 line list to the HITRAN2020 line list.

The recent high-temperature line list from the ExoMol database (named UCL-4000) for the main isotopologue of $CO_2$ ($^{12}C^{16}O_2$) was published in Yurchenko et al. [18]. This line list contains almost 2.5 × $10^9$ transitions involving about 3.5 × $10^6$ states. The wavenumber range of the $CO_2$ list is from 0 to 20,000 $cm^{-1}$ with the lower-state energies up to 16,000 $cm^{-1}$ and $J \leq 202$. These results were generated using UCL's *ab initio* dipole moment surface (DMS) [32] and the semi-empirical potential energy surface (PES) Ames-2 [23] with the variational program TROVE [33]. The UCL-4000 line list was converted to HITRAN format and compared with the HITRAN2016 line list. As a result, more than 3600 spectral lines above 8000 $cm^{-1}$ were added to the HITRAN2020 spectroscopic database [24] (see Section 5).

The NASA Ames line lists for 13 $CO_2$ isotopologues were published by Huang et al. [23]. They were computed at 296 K using the empirically refined Ames-2 potential energy surface and pure *ab initio* DMS-2 dipole moment surface with $J \leq 150$ and the lower-state energy up to 24,000 $cm^{-1}$. Intensities of selected bands from this database were used for HITRAN2020 as described in Sections 2 and 5.

Critical validation tests of the available spectroscopic data were carried out using the existing theoretical and semi-empirical databases, including ExoMol, NASA Ames, and CDSD-296 [17,18,23] and with published experimental works [14,34–42]. Accordingly, the present work allowed revealing some problems with the HITRAN2016 $CO_2$ line list and thus allowed improving and extending the line lists for all 12 stable isotopologues in the final version of the HITRAN2020 $CO_2$ line list.

## 3. Evaluation of the HITRAN $CO_2$ line lists by laboratory and atmospheric spectra

In this section, we present the general review of problematic bands identified in laboratory and atmospheric spectra, mainly those obtained from the Kitt Peak National Observatory, MkIV balloon, CRDS, and TCCON [14–16,38–40]. Most of the issues have been associated with deficient line positions and intensities for which critical validation tests were performed, and alternative sources of data for each problematic band were suggested.

Several $CO_2$ line lists, including HITRAN2008 [43], HITRAN2012 [44], and HITRAN2016 [12], were evaluated by fitting laboratory (mainly Kitt Peak) and atmospheric solar absorption spectra (MkIV and TCCON) between 670 and 8310 $cm^{-1}$ [15,16]. The studied region was divided into several windows, most encompassing at least one complete $CO_2$ absorption band or a sub-branch. The GFIT spectral fitting algorithm [45] was used in all cases assuming a Voigt line profile and no line mixing. The line lists were evaluated in terms of the RMS fitting residuals and the window-to-window consistency of the retrieved gas amounts. There was no analysis of the separate isotopologues. The results showed progressive overall RMS fit improvements through the use of each successive HITRAN version. Fig. 2 shows the absolute RMS residuals of the fits for 41 windows averaged over the 137 Kitt Peak and 12 JPL laboratory spectra in the 670–8310 $cm^{-1}$ spectral region. The pressure range is from 0.013 kPa-93 kPa (0.1 Torr to 700 Torr) except for 2 Kitt Peak spectra (1.71 kPa and 1.89 kPa) covering 600–1400 $cm^{-1}$. However, in this plot, the HITRAN2020 line list gives worse fits in the 3730 $cm^{-1}$ window in Kitt Peak lab spectra than most previous line lists. This is due to the self-broadened half-widths being too small in this region (the Kit Peak lab spectra include some with 200 Torr of pure $CO_2$). This issue has no effect on fits to atmospheric spectra,

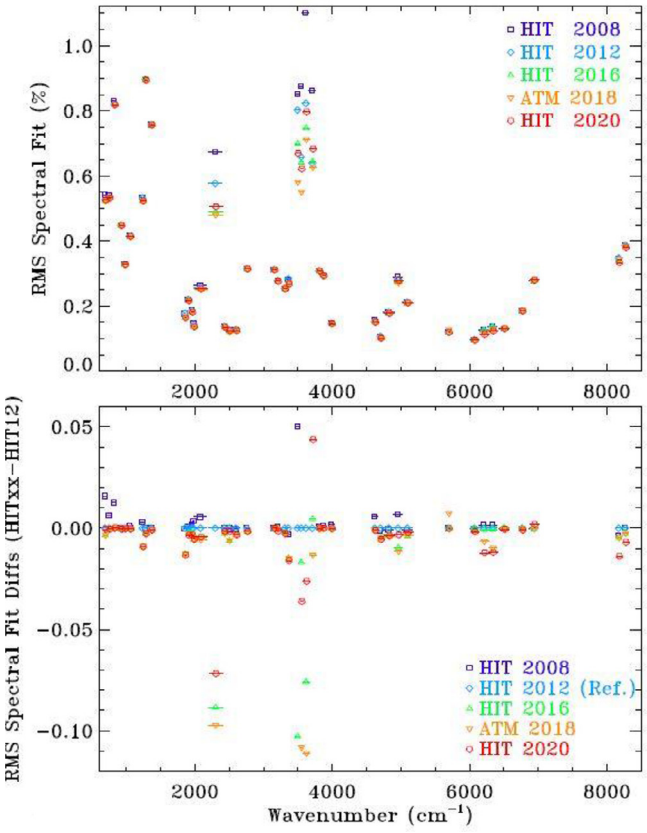


**Fig. 2.** The upper panel shows the absolute value of the mean *RMS* fit for 5 different $CO_2$ line lists: HIT2008: HITRAN2008 [43]; HIT2012: HITRAN2012 [44], HIT2016: HITRAN2016 [12], ATM2018: 523,230 $CO_2$ lines [15], HIT2020: HITRAN2020 [24]. The lower panel shows the differences from HITRAN2012 [44].

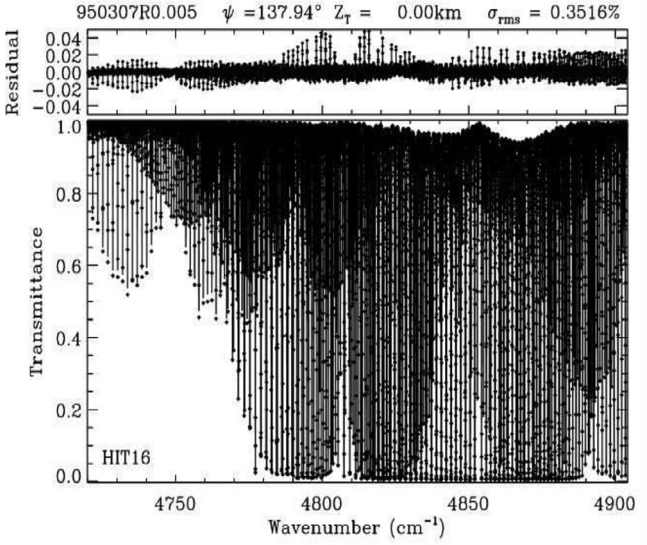


**Fig. 3.** The fits to a Kitt Peak laboratory spectrum in the 4800 $cm^{-1}$ region using the HITRAN2016 linelist [12]. The positive residuals arise from the 40002–01101 band of the $^{12}C^{16}O_2$ isotopologue.

but it will be investigated further. It is also worth noting that the comparisons did not include the line mixing effect, which may also influence the conclusions about the values of self-broadening.

The discrepancies were also identified in the 4800 $cm^{-1}$ regions, where the HITRAN2016 line list was worse than previous editions in terms of RMS fitting residuals. The same situation in

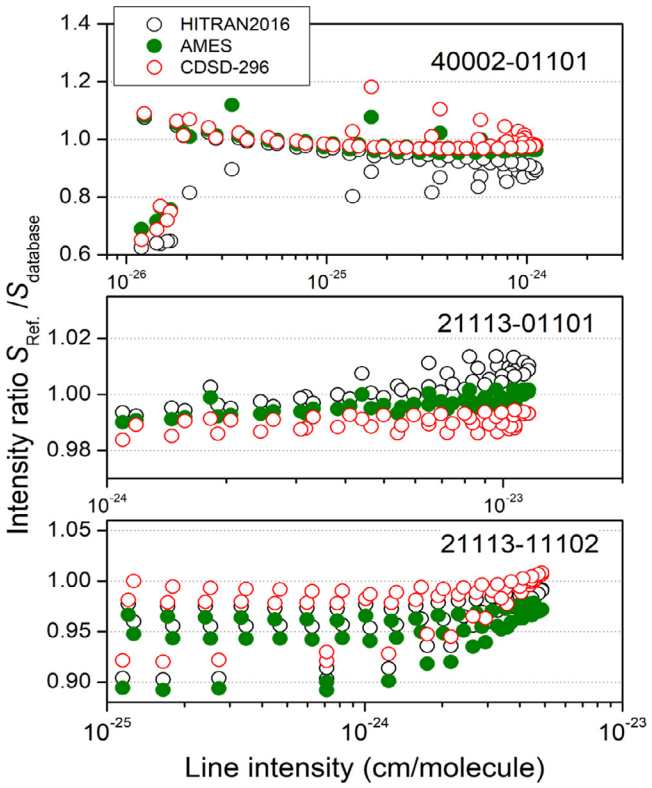


**Fig. 4.** Ratio of the experimental line intensities of the 40002-01101, 21113-01101, and 21113-11102 bands (centers: 4808 $cm^{-1}$, 4809 $cm^{-1}$, and 3544 $cm^{-1}$, respectively) from Refs [34,35] to those from the various $CO_2$ spectroscopic databases [12,17,23].

this region was observed in the MkIV balloon spectra (low pressure). The Kitt Peak laboratory spectrum revealed rotationally-dependent errors at the 10–15% level in the *ab initio* intensities for the 40002–01101 band of the $^{12}C^{16}O_2$ isotopologue. Fits to a Kitt Peak laboratory spectrum in the 4800 $cm^{-1}$ region are presented in Fig. 3. Also, it was shown that the scattering factor of the 40002–01101 band is slightly elevated (1.4 to 1.7). In addition to that, for low $J$, around $J = 1$ to 3, there is a visible spike in the scatter factor, which suggests a $J$-localized resonance. Indeed, by analyzing predictions within the effective operator model [30], it was found that the 40002 and 21113 vibrational levels of the $P = 8$ polyads are interacting through a Coriolis interaction. This interaction causes systematic problems with the *ab initio* intensities [27] for the transitions involving either of these two vibrational states.

For the HITRAN2016 $CO_2$ line list, there are 24 bands involving the 40002 and 21113 vibrational levels affected by Coriolis interaction. To quantify the impact of this perturbation on intensities, validation tests for the 40002-01101, 21113-01101, and 21113-11102 bands of the $^{12}C^{16}O_2$ isotopologue were carried out using the published experimental values [34,35] and data from the various carbon dioxide spectroscopic databases [12,17,23] (Fig. 4). This comparison showed that the CDSD-296 line intensities [17] are preferable for the 40002-01101 and 21113-11102 bands whereas, in the case of the 21113–01101 band, the *ab initio* intensities from NASA Ames [23] are the best choice. However, because of the lack of measurements, we could not make similar comparisons for the numerous remaining bands affected by these Coriolis interactions. We hope that new experimental data will become available for further validation tests of bands involving the 40002 and 21113 vibrational levels.

In the 1800–2000 $cm^{-1}$ spectral region, $CO_2$ retrievals of mixing ratio based on the HITRAN2016 database produces $CO_2$ retrieved amounts that are 5% larger than those based on previous line lists. The VMR Scale Factors (VSF) obtained by averaging each retrieved single-spectrum VFS value over all 19 MkIV balloon spectra that were fitted for each window are plotted versus wavenumber in Fig. 5. The MkIV instrument simultaneously records the region 600 $cm^{-1}$ to 5650 $cm^{-1}$, so derived VSFs should have good window-to-window consistency.

It was found that the most significant deviations in this region correspond to the 11102-00001 band near 1933 $cm^{-1}$. The 11101-00001 and 11102-00001 bands borrow intensities from the strong 00011-00001 band *via* Coriolis interaction. It was shown in

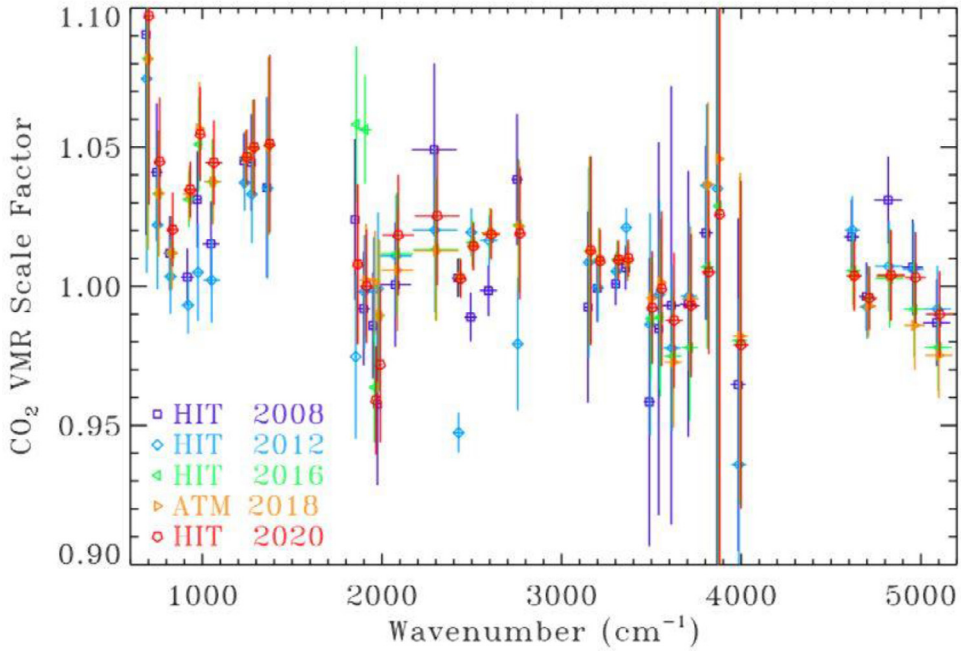


**Fig. 5.** The VMR Scale Factors (VSF) were obtained by averaging each retrieved single-spectrum VFS value over all 19 MkIV balloon spectra that were fitted for each window. The measured VSF values are plotted versus wavenumber. See the designations of the databases in the caption of Fig. 2.

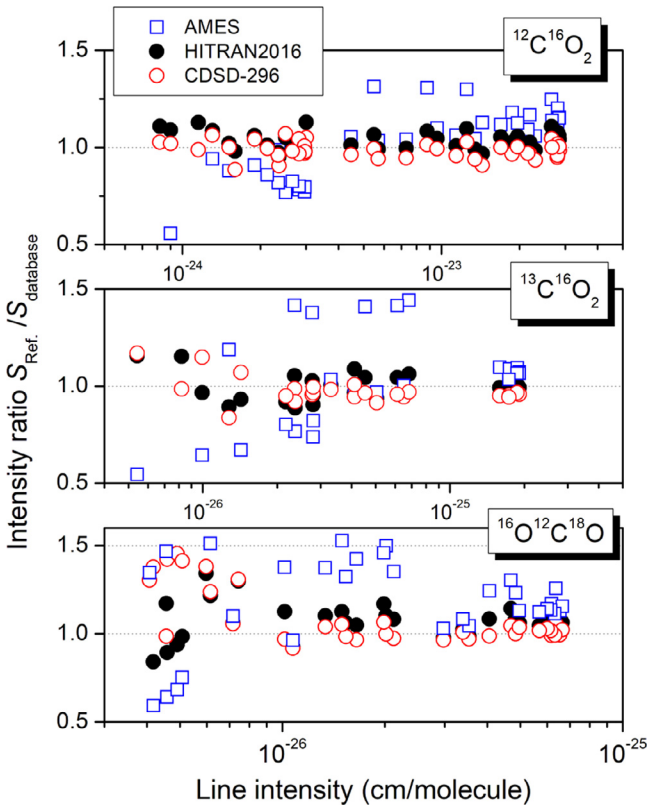


**Fig. 6.** The comparison of line intensities between the published measurements from Refs [36,37] and the different $CO_2$ databases [12,17,23] for the 11102–00001 bands of the $^{12}C^{16}O_2$, $^{13}C^{16}O_2$, and $^{16}O^{12}C^{18}O$ isotopologues with centers: 1933 $cm^{-1}$, 1897 $cm^{-1}$, and 1903 $cm^{-1}$, respectively.

Ref. [17] that the *ab initio* NASA Ames line intensities [23] for the 11101-00001 band deviate considerably from the observations. A comparison of the 11102-00001 line intensities with the published measurements [36,37] and the different $CO_2$ databases [12,17,23] for the $^{12}C^{16}O_2$, $^{13}C^{16}O_2$, and $^{16}O^{12}C^{18}O$ isotopologues is presented in Fig. 6. Replacement of line intensities of the $CO_2$ bands considered in the HITRAN2016 database with CDSD-296 [17] rectifies the above-mentioned discrepancy in the 1800–2000 $cm^{-1}$ region. For consistency, the line intensities of the 11101-00001 band for other $CO_2$ isotopologues were also replaced by the intensities from the CDSD database in the HITRAN2020 line list. The 20003–01101 and 12202–01101 hot bands of $^{12}C^{16}O_2$ located near 1900 $cm^{-1}$ were also increased by 5% to match the ATM values [15]. The intensity origin for these bands in HITRAN2016 are: 20003–01101 – UCL *ab initio* [27] and 12202–01101 – UCL *ab initio* and CDSD2015 [26,27].

The TCCON observations considered here cover the 3950 to 9500 $cm^{-1}$ spectral region. These measurements are made with a Fourier transform spectrometer with an InGaAs detector and optical path difference (OPD) of 45 cm, corresponding to a resolution of 0.02 $cm^{-1}$. We use the definition: resolution = 0.9/OPD, which is how the Bruker OPUS software defines it. This assumes that the interferograms have been windowed with a Triangular, Happ-Genzel, or Blackman-Harris apodization function. For a box-car apodization (i.e. no apodization), the resolution would be 0.61/OPD. Use of the HITRAN2016 line lists reduces the $CO_2$ retrieved from the 6220 and 6338 $cm^{-1}$ windows by 0.5% and 1.5%, respectively, by comparison to results obtained with the other line lists, thus introducing a new inconsistency of 1.5%. Retrieved VMR Scale Factors (VSF) obtained by averaging single-spectrum based on fitting each spectral window from the TCCON spectra are presented in Fig. 7. This issue is associated with the 30012-00001 and 30013-00001 line parameters and is discussed in detail in Section 4.

The comparison of the fits to 136 Kitt Peak lab spectra with those modeled using the HITRAN2016 $CO_2$ line list shows large residuals in the 3500 and 4800 $cm^{-1}$ spectral windows due to inaccuracies of line positions of the 10012–00001, 20012–00001, and 20013–00001 bands of the $^{13}C^{16}O_2$ isotopologue. It was shown that the HITRAN2012 [44] line positions for the 20012–00001 and 20013–00001 bands led to better residuals than those of the HITRAN2016 and CDSD-296 [17] databases. As a result, the line positions of the 20012-00001 and 20013-00001 bands of the $^{13}C^{16}O_2$ isotopologue were replaced with the corresponding HITRAN2012 line positions in the HITRAN2020 $CO_2$ line list. In the case of the 10012–00001 band, we subtracted 0.0009 $cm^{-1}$ from the CDSD [17] line positions used for this band in HITRAN2020 to match the ATM values [15].

Also, inaccuracies in the positions of some $^{16}O^{12}C^{18}O$ lines of the 01121–01101 hot band (P13e, P14e, P14f, Q12f, Q13e, Q13f, R11e, R12e, and R12f) were evidenced in the HITRAN2016 line list between 4600 and 4625 $cm^{-1}$. This issue was identified by comparison with fits to Kitt Peak spectra and was solved by replacing the line positions with positions from the CDSD-296 database [17] in the HITRAN2020 $CO_2$ line list.

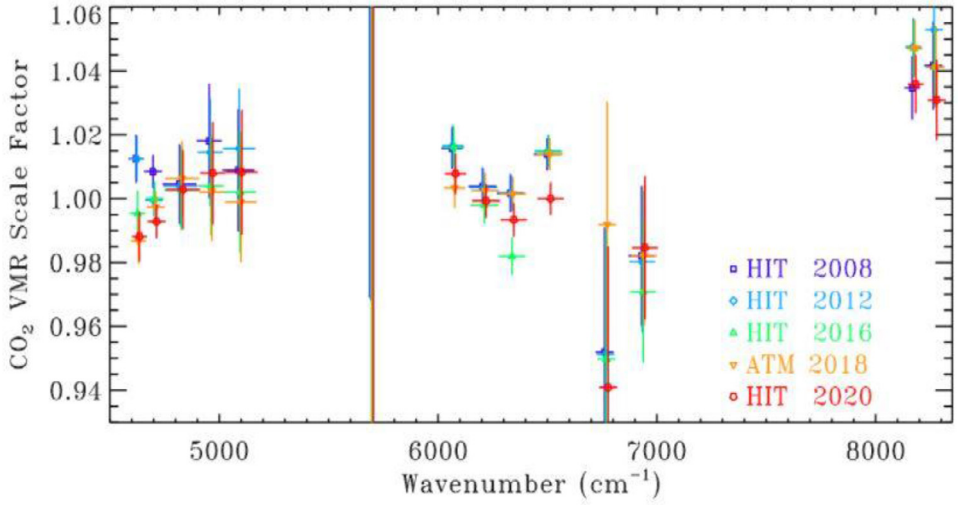


**Fig. 7.** Retrieved VMR Scale Factors (VSF) obtained by averaging single-spectrum based on fitting each spectral window from the TCCON spectra. Results are plotted versus wavenumber. See the designations of the databases in the caption of Fig. 2.

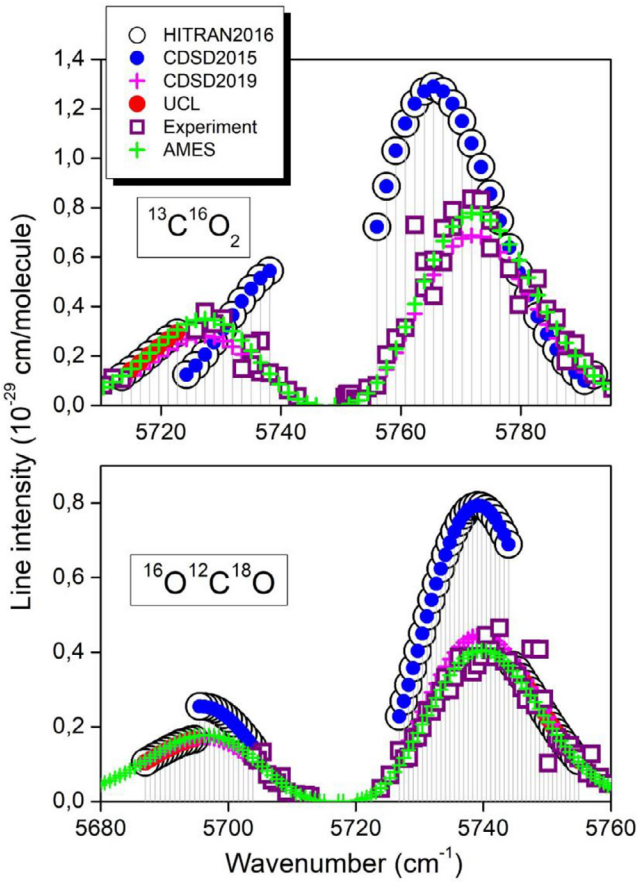


**Fig. 8.** Comparison of the CRDS measurements (purple squares) of the 41104-00001 band of $^{13}C^{16}O_2$ [46] and $^{16}O^{12}C^{18}O$ [40] to various databases: HITRAN2016 [44], CDSD-296 (CDSD2015) [26], CDSD-296 (CDSD2019) [17], UCL [27,28], and NASA Ames [23] line lists.

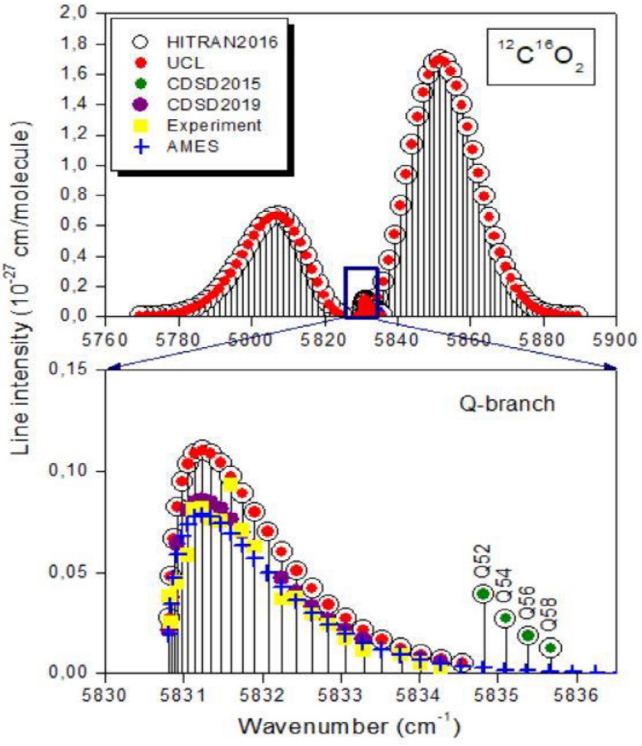


**Fig. 9.** Overview comparison of the Q-branch of the 41104-00001 band ($^{12}C^{16}O_2$) [39] to the HITRAN2016 [12], CDSD-296 (CDSD2015) [26], CDSD-296 (CDSD2019) [17], UCL [27] and NASA Ames [23] line lists. The lower panel highlights the Q-branch where the HITRAN2016 list uses UCL and CDSD2015 as intensity sources for *J* below 50 and above 52, respectively, leading to the observed intensity jump between Q(50) and Q(52). The CRDS measurements [39] validate the NASA Ames intensity values which were taken as the unique source for HITRAN2020 of this band.

As mentioned above, below 8000 cm$^{-1}$, most line intensities in the HITRAN2016 database came from the UCL-IAO line lists [27–29] which are based on *ab initio* calculations. Because of excessive uncertainty in the *ab initio* line positions, the HITRAN2016 line list is, in general, a combination of the CDSD- based line positions [26] and the UCL variational line intensities [27–29]. In the case of the so-called "sensitive bands" (as defined by Zak et al. [27–29]) *ab initio* intensities were replaced with those from CDSD when available. This substitution resulted in some cases where transitions in a given band would have intensities from both *ab initio* calculations as well as those from CDSD. Although this approach was justified in many cases, a number of inconsistencies in the rotational distribution of intensities in HITRAN2016 were revealed in CRDS spectra of $^{18}O$ and $^{13}C$ enriched and natural $CO_2$ near 1.74 μm [39,40,46]. In these works, the anomalies involve the perpendicular bands of the $\Delta P = 9$ series of transitions. As shown in Fig. 8, the mixing of CDSD and UCL *ab initio* intensities for the 41104–00001 bands of $^{12}C^{16}O_2$ and $^{13}C^{16}O_2$ isotopologues leads to an apparent inconsistency in the rotational dependence with substantial intensity variation between successive *J* values or even missing transitions. A similar situation was found in the case of the 41104–00001 band of $^{16}O^{12}C^{18}O$ isotopologue (See Fig. 9). A comparison of the measurements from Refs [39,40,46] to various carbon dioxide spectroscopic databases is presented in Fig. 10. As can be seen from this figure, the NASA Ames intensity values for this band are all close to the experimental ones. As a result, for HITRAN2020, the NASA Ames intensities of the 41104–00001 bands of the $^{12}C^{16}O_2$, $^{13}C^{16}O_2$, and $^{16}O^{12}C^{18}O$ isotopologues were preferred to the mixed intensity values in the HITRAN2016 line list.

Similar validation tests using the values available in the literature and from the different $CO_2$ databases were carried out for other bands affected by the problem due to the mixing of intensities of CDSD and *ab initio* origin in the HITRAN line list. These bands were systematically searched (see Fig. 5 of Ref. [39]), and when problems were identified, alternative sources of data for each such band were suggested. For the $^{12}C^{16}O_2$, $^{13}C^{16}O_2$, $^{16}O^{12}C^{18}O$, and $^{16}O^{13}C^{18}O$ isotopologues, we present in Table 1 the set of bands that were checked and affected by this issue along with the alternative intensity sources for these bands used in HITRAN2020. The substitution of the suggested intensity sources for the bands presented in Table 1 was performed for the corresponding bands of all the $CO_2$ isotopologues in HITRAN2020 where experimental data exists. In the absence of experimental reference data, the replacement of the intensity source was performed only for the corresponding band of the specific isotopologue. In the case of the 31104e-01101e and 11112e-11101e hot bands of the $^{16}O^{12}C^{18}O$ and $^{13}C^{16}O_2$ isotopologues, respectively (see Fig. 11), we cannot offer an alternative source for replacing the mixed line intensities, since there is no experimental data to verify them. Nevertheless, we kept the HITRAN2016 line intensities for the 31114e-01101e band of $^{16}O^{12}C^{18}O$ isotopologue in HITRAN2020. In the future, we will consider using UCL *ab initio* [28] line intensities for this band. In the case of the 11112e-11101e hot band of the $^{13}C^{16}O_2$ isotopologue, the UCL and CDSD-296 databases [17,27] give similar line intensities, although there is an inconsistency in the rotational dependence with substantial intensity variation between successive *J* values of the P-branch. Validation of this band is a challenge for fu-

**Table 1**
The bands for the $^{12}C^{16}O_2$, $^{13}C^{16}O_2$, $^{16}O^{12}C^{18}O$, and $^{16}O^{13}C^{18}O$ isotopologues where intensities were from mixed sources in HITRAN2016 and the new sources of intensities chosen for HITRAN2020.

| Band | Band center ($cm^{-1}$) | Intensity origin | | Experimental works |
|---|---|---|---|---|
| | | HITRAN2016 | HITRAN2020 | |
| $^{12}C^{16}O_2$ isotopologue | | | | |
| 21103–02201 | 1846.33 | [26,27] | [26,27] | – |
| 13302–02201 | 1907.85 | [26,27] | [27] | – |
| 20002–01101 | 2003.76 | [26,27] | [17] | [41] |
| 21102–10002 | 2054.72 | [26,27] | [27,28] | – |
| 22201–11101 | 2120.50 | [26,27] | [17] | [42] |
| 40002–21103 | 2295.65 | [26,27] | [27] | – |
| 30004–01101 | 3125.10 | [26,27] | [17] | [34] |
| 31104–10002 | 3131.52 | [26,27] | [27] | – |
| 22203–01101 | 3156.20 | [26,27] | [27] | – |
| 31103–10002 | 3306.48 | [26,27] | [27] | – |
| 22202–01101 | 3342.10 | [26,27] | [27] | – |
| 23302–02201 | 3344.01 | [26,27] | [27] | – |
| 31102–10001 | 3365.31 | [26,27] | [17] | [34] |
| 30002–01101 | 3398.45 | [26,27] | [27] | – |
| 21101–00001 | 3501.45 | [26,27] | [27] | – |
| 40002–11102 | 3544.64 | [26,27] | [27] | – |
| 01121–10002 | 4031.07 | [26,27] | [27] | – |
| 31104–00001 | 4416.15 | [26,27] | [17] | [35] |
| 41103–10001 | 4613.12 | [26,27] | [27] | – |
| 25501–02201 | 4696.61 | [26,27] | [27] | – |
| 10021–01101 | 5346.31 | [26,27] | [17] | [47] |
| 50006–01101 | 5572.65 | [26,27] | [27] | – |
| 50005–01101 | 5768.12 | [26,27] | [27] | [39] |
| 42204–01101 | 5805.64 | [26,27] | [17] | [39] |
| 41104–00001 | 5830.79 | [26,27] | [23] | [39] |
| 50004–01101 | 5920.94 | [26,27] | [27] | – |
| 50003–01101 | 6057.89 | [26,27] | [27] | [48] |
| $^{13}C^{16}O_2$ isotopologue | | | | |
| 04421–01101 | 1946.12 | [26,29] | [27,28] | – |
| 11112–11101 | 2110.13 | [26,27] | [27] | – |
| $^{16}O^{12}C^{18}O$ isotopologue | | | | |
| 31104–30004 | 616.12 | [26,28] | [17,28] | – |
| 21101–10002 | 2195.21 | [27,28] | [28] | – |
| 21101–00001 | 3454.63 | [27,28] | [28] | – |
| 31104–01101 | 3677.44 | [26,28] | [28] | – |
| $^{16}O^{13}C^{18}O$ isotopologue | | | | |
| 12202–01101 | 1856.75 | [26,28] | [28] | – |

ture experiments. It should also be noted that for the 21103-02201 band of the $^{12}C^{16}O_2$ isotopologue in Table 1, the line intensity was updated only for the R2e line from CDSD2015 [26] to UCL [27] in HITRAN2020. This is the reason why the source of the line intensity remained the same as in HITRAN2016.

## 4. New experimental data with sub-percent uncertainty

Accurate line parameters of the spectral lines are generally required for the most demanding atmospheric applications. In particular, the accurate values of the line intensities with uncertainties as low as 0.3%–0.5% [49] are necessary for forward models used in retrievals of $CO_2$ concentrations from some remote sensing missions. A number of very accurate measurements have become available after the release of HITRAN2016 in the NIR region: the most recent CRDS measurements from NIST [19,20] and FTS measurements from DLR reported in Birk et al. [22] (with the corresponding measurements and line parameter database provided on Zenodo [21]). The results obtained in these works were used to improve the HITRAN line intensities of the $^{12}C^{16}O_2$ isotopologue.

The accurate CRDS line intensity measurements for the 3001*i*–00001 ($i = 2$–4) bands reported by Long et al. [19] were used to refine the calculated HITRAN2016 $CO_2$ band intensities near 1.6 $\mu$m. This region is actively used for spectroscopic measurements of atmospheric $CO_2$ concentrations. For instance, the 30013–00001 band is targeted by the OCO-2 and OCO-3 missions [5,7], while the 30012–00001 band is used for the LIDAR missions [50]. It was shown in Ref. [19] that the band-integrated CRDS intensity measurements and the *ab initio* calculations of Zak et al. [27] agree at the 0.06% level for the 30013–00001 and 30014–00001 bands, but there is a systematic discrepancy of about 1.1% for the 30012–00001 band. We note that the HITRAN2016 line intensities are from the *ab initio* UCL results [27], and they have relative uncertainties < 2% for the 30012-00001 and 30013-00001 bands and < 5% for the 30014-00001 band, respectively. In contrast, the current $CO_2$ spectroscopic databases [17,23] show a significant spread in their line intensities at about or above 1%. Following these results [19], the HITRAN2016 line intensities for the 3001*i*–00001 ($i = 2$–4) bands were scaled to the recommended band-dependent scaling constant factors, while preserving the original *J*-dependence of the *ab initio* calculations. The comparison of the HITRAN2016 and HITRAN2020 line intensities of the 30012–00001 band of $^{12}C^{16}O_2$ isotopologue to the experimental values reported in Long et al. [19] is plotted in Fig. 12.

Bruker IFS 125HR Fourier-transform spectrometer measurements have been conducted at the German Aerospace Center (DLR) to measure pure carbon dioxide transmittance spectra in the 6000–7000 $cm^{-1}$ spectral region, including the 30011-00001,

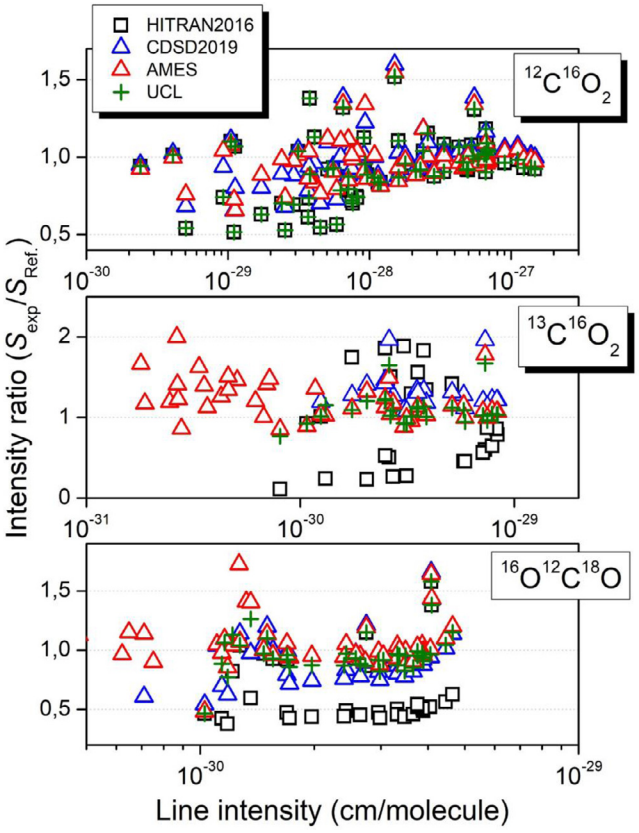


**Fig. 10.** Ratios of the measured line intensities of the 41104-00001 band of the $^{12}C^{16}O_2$, $^{13}C^{16}O_2$ and $^{16}O^{12}C^{18}O$ [39,40,46] isotopologues to the HITRAN2016 [12], CDSD-296 (CDSD2019) [17], UCL [27,28], and NASA Ames [23] line lists.

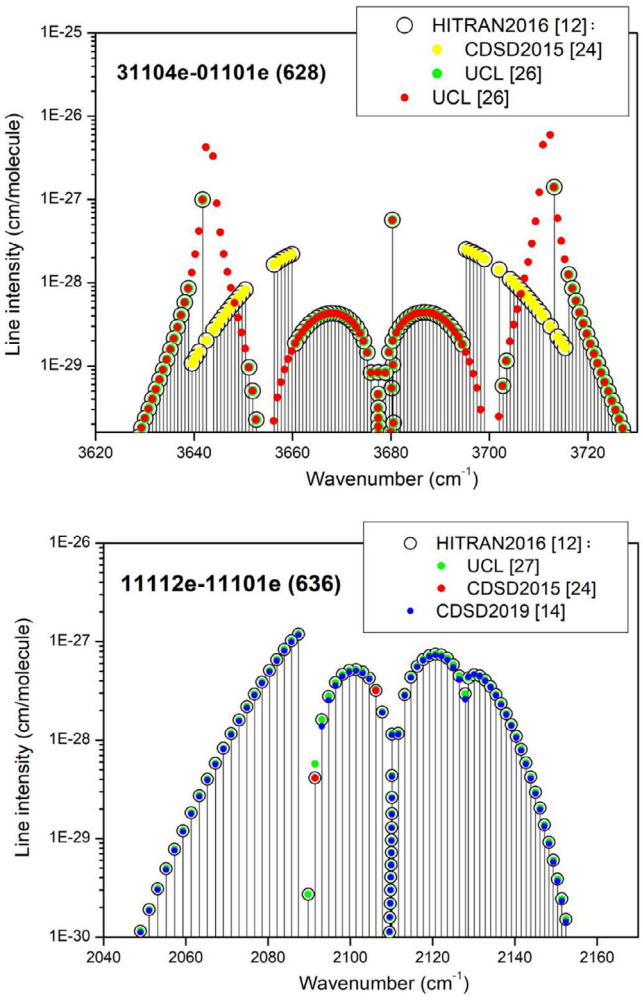


**Fig. 11.** The 31104e-01101e and 11112e-11101e hot bands of the $^{16}O^{12}C^{18}O$ (628) and $^{13}C^{16}O_2$ (636) isotopologues, respectively, having the mixed line intensities in the HITRAN2016 database [12].

30012-00001, 30013-00001, 30014-00001, and 00031-00001 bands [22]. In this work, line intensity uncertainties of 0.15% were reported. The scaling factor 1.0061 was used for the HITRAN2016 line intensities of the 30011-00001 band of the $^{12}C^{16}O_2$ isotopologue to match with DLR measurements [22]. The 30013-00001 and 30014-00001 HITRAN2016 line intensities and NIST measurements were found to be in good agreement with the DLR measurements. However, for the 30012-00001 band, the differences outside of the stated uncertainties with both NIST measurements and HITRAN2016 were reported. The difference for the 30012–00001 band was 1.6%, whereas for Long et al. [19] the difference was about 1%. It should be noted that these differences are outside the stated uncertainty budget. In addition, the DLR data showed systematic differences of relative line intensities to HITRAN2016 within the 3001$i$-00001 ($i$ = 2,3) bands on the order of 0.3%.

Regarding the line positions for the 3001$i$–00001 ($i$ = 2–4) bands, they were replaced with positions from the CDSD-296 database [17] in the HITRAN2020 line list (See Section 2 for details).

As an example, we will refer to two recent papers [51,52] that provide a comparison for line positions of the 30012–00001 and 30013–00001 bands. These works confirm good agreement of the line positions for the corresponding bands with an experimental measurement [53-58] and the CDSD-296 [17] database. The comparison for the 30012–00001 line positions with the known and most recent measurements [51,53-55] is given in Fig. 6 of Ref. [51], including CDSD-296 [17]. This figure shows that the accurately measured line positions [51] to those from Refs [53-55] agree reasonably well for the quantum number below −32. However, it does not include the comparison with the recently measured P32 transition from Ref. [56] with the 120 kHz uncertainty, but this position value equals 6319.195652 $cm^{-1}$ (fitted by Voigt profile) and totally coincides with the position value of P32 transition from Ref. [51] used in Fig. 6. Lamb dips of the 30013–00001 line positions were accurately measured by a comb-locked cavity ring-down spectrometer with an accuracy of a few kHz. Fig. 5 in Ref. [52] shows the comparison of line positions obtained in Ref. [52] and those reported by Long et al. [57] with Doppler-limited, and by Burkart et al. [58] with Doppler-free, Lamb-dip measurements. The comparison with CDSD-296 [17] is also presented that agree very well with measurements with differences around 20 kHz for $-44 \le m \le 43$, and the difference increases up to 4.6 MHz for $J = 72$.

In Fleurbaey et al. [20], it was shown that a constant scaling of 1.0069±0.0002 of HITRAN2016 values in the 20013–00001 band of $CO_2$ near 2.06 $\mu$m is consistent with the experiment. Therefore, we have performed this scaling in HITRAN2020. In Refs [19,20], the reported relative uncertainty in intensity is better than 0.1%, thus the uncertainty code 8 (< 1%) for the line intensities was given for the corresponding bands in the HITRAN2020 line list.

In the HITRAN2016 edition, the line intensities of the 00031–00001 band of the $^{12}C^{16}O_2$ isotopologue near 1.4 µm used CDSD-296 [26] as an intensity source because this band was identified as "sensitive" in the *ab initio* calculations [27]. The comparison of the CDSD line intensities with the DLR measurements [20] showed rotationally-dependent deviations up to 4%. To improve the 00031–

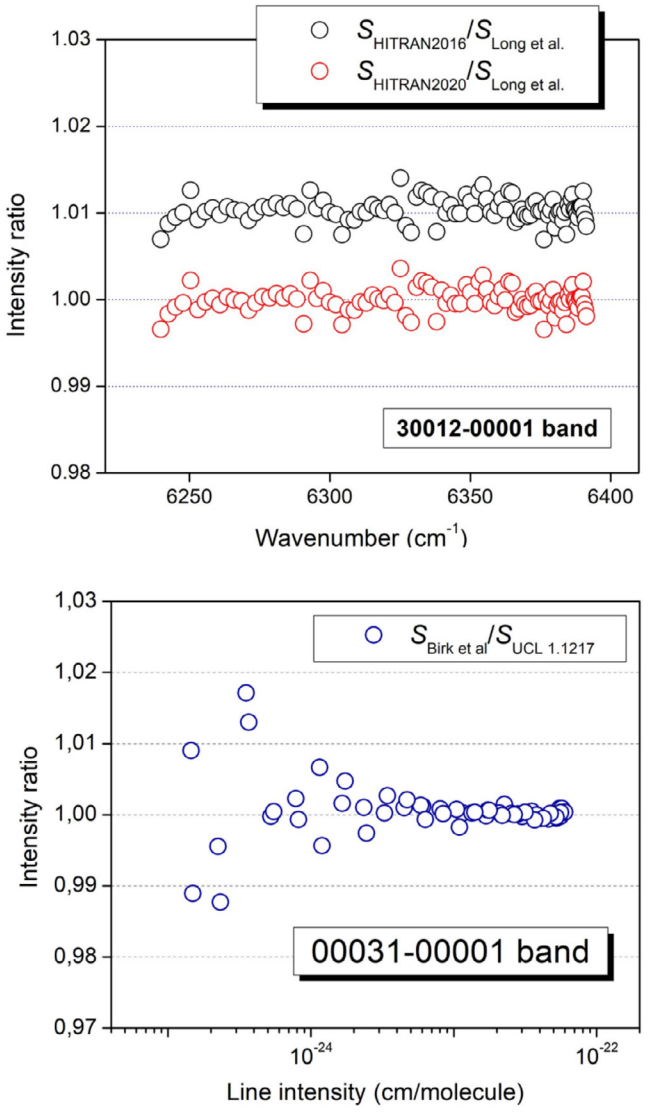


**Fig. 12.** *Upper panel:* Comparison of the HITRAN2016 and HITRAN2020 line intensities of the 30012–00001 band of $^{12}C^{16}O_2$ isotopologue to the experimental values measured by Long et al. [19]. *Lower panel:* Comparison of the measured line intensities reported in Birk et al. [22] and the UCL intensities scaled by the factor of 1.1217 for the 00031–00001 band of the $^{12}C^{16}O_2$ isotopologue. Scaled UCL intensities were adapted for HITRAN2020 in this band.

00001 line intensities in the HITRAN2020 line list, we scaled the UCL line intensities [27] by the factor of 1.1217 to match the line intensities reported by Birk et al. [22] (See Fig. 12). It should be noted that two lines (P20 and R18) were absent in the UCL line list [27], so that the intensities of these corresponding lines were updated from Birk et al. [22].

The weak 10032-10002 and 01131-01101 hot bands of the $^{12}C^{16}O_2$ isotopologue located near 6900 cm$^{-1}$ were also compared to the DLR measurements [22]. It was found that the HITRAN2016 line intensities of the 10032-10002 band should be scaled by a factor of 1.1346 while the line intensities of the 01131-01101 band having the intensity origin from CDSD-296 K [26] should be scaled by a factor of 1.0022.

## 5. New bands above 8000 cm$^{-1}$

The recent high-temperature ExoMol UCL-4000 line list containing almost 2.5 × 10$^9$ transitions at $T$ = 4000 K for the $^{12}C^{16}O_2$ isotopologue was published in Ref. [18]. To compare this line list with HITRAN2016, we converted UCL-4000 to HITRAN format at 296 K and applied an intensity cut-off of 10$^{-30}$ cm/molecule using the ExoMol_to_HITRAN.py program downloaded from http://exomol.com/software/ [59]. This code transfers the position, intensity, Einstein A, lower state energy, and upper/lower level statistical weights into the correct location for a HITRAN default format ".par" file. It works by looking at the "trans" file to get the upper and lower state ID. We edited this program to extract the $m_1$, $m_2$, $l_2$, $m_3$ HITRAN quantum numbers from the ExoMol files. In the case where the states were not assigned, the vibrational assignments were replaced with "–2–2–2–2". When it was possible, we also performed additional assignments using the CDSD-296 [17] and Ames [23] databases. Fig. 13 gives an overview comparison of the HITRAN2016 line list to the UCL-4000 line list for the $^{12}C^{16}O_2$ isotopologue from 0 to 20,000 cm$^{-1}$. It should be noted that the $^{12}C^{16}O_2$ line list in HITRAN2016 was limited to the spectral range 158.302 to 14,075.298 cm $^1$. The new $^{12}C^{16}O_2$ lines from the UCL-4000 line list, along with data from the HITRAN2016 database, are shown in Fig. 13. These UCL-4000 transitions are highlighted in blue and located above 8000 cm$^{-1}$. Over 3600 spectral lines with line intensities from 1.8 × 10$^{-28}$ to 9.9 × 10$^{-30}$ cm/molecule from the UCL-4000 line list were included in the HITRAN2020 spectroscopic database. The line positions in the UCL-4000 dataset [18] are calculated from the energy levels derived from the HITRAN2016 database. Due to the diversity of data in HITRAN some inconsistencies could occur when deriving upper state energy levels, which could result in deviations. As a result, the UCL-4000 line list has an issue regarding the matching of line positions. As an example, this case is shown in Fig. 14, where the comparison of the line positions for the 50015-00001 and 60014-10002 bands of the $^{12}C^{16}O_2$ isotopologue is presented. We traced the source of the discrepancies in UCL-4000 to the procedure used to substitute the variational (upper) state energies with the empirical values. The substituted energies were taken from HITRAN2016, either as the lower state energy term values E" or as E' = E" + $\nu$ (where $\nu$ is the transition wavenumber). The examples of these upper state energies, including those shown in Fig. 14, were affected by the inconsistency of the original line positions from different sources. Most of such inconsistency cases identified in the present analysis have been improved in HITRAN2020 and will be propagated to UCL-4000 after the release of HITRAN2020.

The weak 30022-00001 and 30023-00001 bands of the $^{16}O^{12}C^{18}O$ isotopologue with band centers as 8374.23 cm$^{-1}$ and 8497.45 cm$^{-1}$, respectively, were missing in the HITRAN2016 [12] and CDSD-296 [17] spectroscopic databases. These bands were assigned in the analysis of CRDS spectra of natural $CO_2$ near 1.18 μm [14] and included in the new $CO_2$ line list. We also calculated the energy levels (thereby obtaining line positions) for the 30022-00001 and 30023-00001 bands of $^{16}O^{12}C^{18}O$ up to $J_{max}$=34 using the spectroscopic constants of the lower and upper state obtained in Refs [14,60] and Eq. (1).

$$F_v(J) = G_v + B_vJ(J+1) - D_vJ^2(J+1)^2 + H_vJ^3(J+1)^3 \quad (1)$$

where $G_v$ is the vibrational term value, $B_v$ is the rotational constant, $D_v$ and $H_v$ are the centrifugal distortion constants, $J$ is the angular momentum quantum number.

Also, it was shown in Ref. [14] that the R-branch intensities of the very weak 00041-01101 hot band of the $^{12}C^{16}O_2$ isotopologue, which are missing in CDSD-296 [17], are in good agreement with the NASA Ames intensities [23] while HITRAN2016 values were largely overestimated. For the HITRAN2020 database, the line intensities of the 30022–00001, 30023–00001, and 00041–01101 bands were updated using the line intensities from NASA Ames [23]. Fig. 15 shows the good agreement between the CRDS line intensities from Ref. [14] and the calculated values from the NASA Ames line list [23]. The uncertainty codes for line positions and

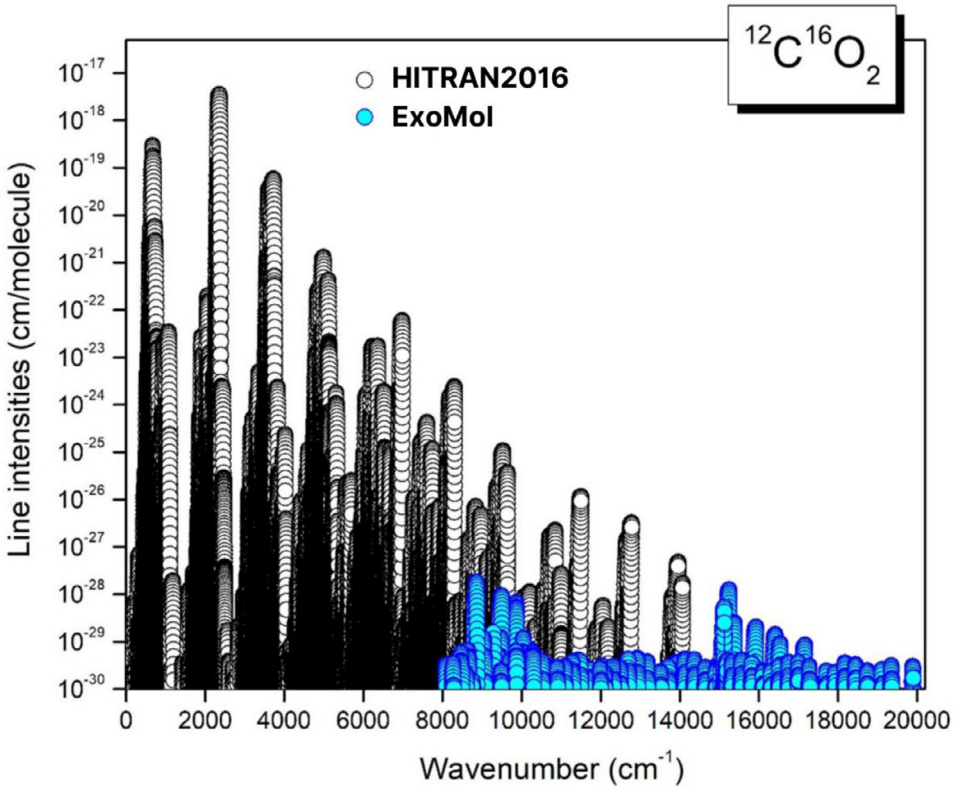


**Fig. 13.** Overview of the HITRAN2020 line list for principle isotopologue in the 0–20,000 cm$^{-1}$ spectral region. Bands that also existed in HITRAN2016 [12] are shown in black and those added from ExoMol UCL-4000 [18] are shown in blue.

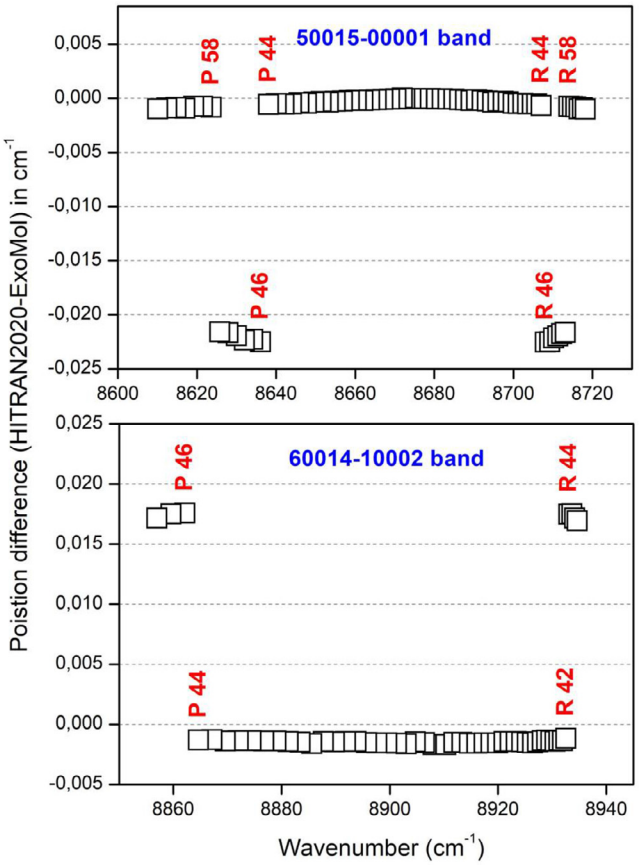


**Fig. 14.** Difference between the HITRAN2020 and ExoMol UCL-4000 line positions for the 50015-00001 and 60014-10002 bands of the $^{12}C^{16}O_2$ isotopologue.

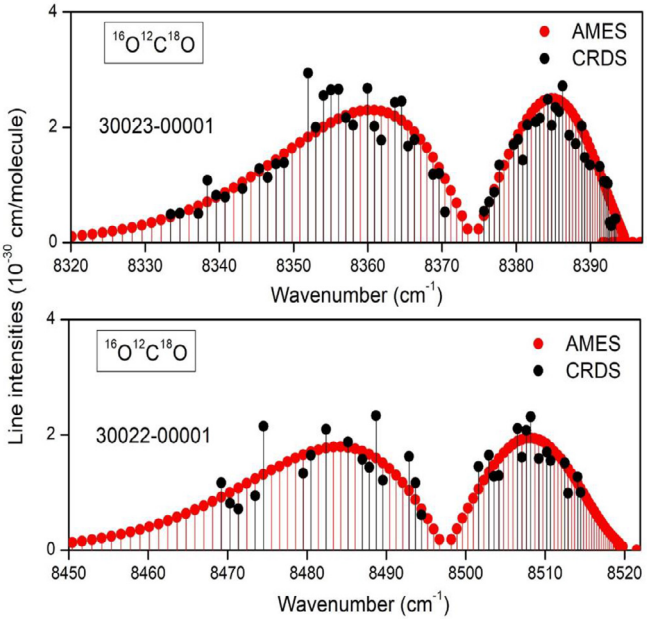


**Fig. 15.** Comparison CRDS [14] and NASA Ames [23] line intensities of the 30022-00001 and 30023-00001 bands of the $^{16}O^{12}C^{18}O$ isotopologue.

intensities were updated to 4 for these bands in the HITRAN2020 line list, corresponding to ($\geq$ 0.0001 cm$^{-1}$ and $<$ 0.001 cm$^{-1}$) and ($\geq$ 10% and $<$ 20%), respectively.

## 6. Addition of magnetic dipole band of $^{12}C^{16}O_2$ at 3.3 μm

The HITRAN2020 database has been extended by including the 01111-00001 ($\nu_2+\nu_3$) magnetic dipole band of the principal iso-

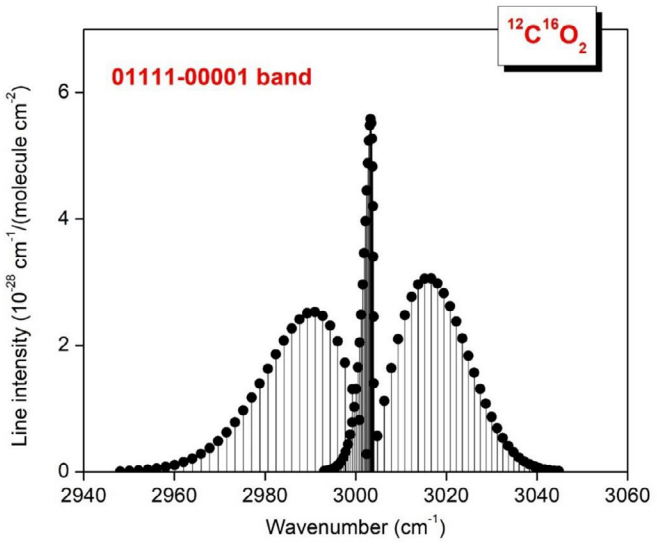


**Fig. 16.** The 01111–00001 magnetic dipole band of the main $CO_2$ isotopologue [64,66]. The band center of this band is 3004.012 cm$^{-1}$.

topologue of carbon dioxide. These line parameters were introduced into HITRAN for the first time; all previous editions of HITRAN provided only $CO_2$ electric dipole transitions. Interestingly, the first observation of the $\nu_2+\nu_3$ band has been reported at 3.3 μm in the atmosphere of Mars [61] by the ExoMars Trace Gas Orbiter ACS instrument [62]. This band is forbidden as an electric dipole absorption. However, it is allowed through electric quadrupole and the magnetic dipole mechanisms, which are typically much weaker than those allowed through the electric dipole mechanism. The maximum line intensities in the 01111–00001 band are on the order of $6 \times 10^{-28}$ cm/molecule. The detailed studies of this band providing the selection rules for the vibration-rotation transitions are presented in Refs [61,63]. The vibrational transition magnetic dipole moment of the 01111–00001 band was fitted to the line intensities measured with a Bruker IFS 125 HR FTS and a 30 m base multipass gas cell of the V.E.Zuev Institute of Atmospheric Optics SB RAS [64]. The line positions and intensities of this band were computed using the vibrational transition magnetic dipole moment and the set of the effective Hamiltonian parameters reported by Majcherova et al. [65]. We included the calculated line parameters up to $J = 64$ of the 01111–00001 band of $^{12}C^{16}O_2$ in the HITRAN2020 line list. The calculated line intensities were consistent with an intensity cut-off $10^{-30}$ cm/molecule at 296 K. The calculated line intensities agree well with the values measured independently by Optical-Feedback-Cavity Enhanced Absorption Spectroscopy (OFCEAS) in Fleurbaey et al. [66] for five R-branch lines of this band (R26-R32 and R36). An overview of the 01111–00001 magnetic dipole band of the main $CO_2$ isotopologue with band center 3004.012 cm$^{-1}$ is displayed in Fig. 16. The corresponding uncertainty codes for the line positions and intensities were used for the 01111–00001 band of $^{12}C^{16}O_2$: code 4 ($\geq$ 0.0001 and $<$ 0.001) and code 4 ($\geq$ 10% and $<$ 20%), respectively. It should be noted that to distinguish the magnetic dipole transitions in the traditional HITRAN ".par" format, the letter "m" was introduced into the quantum field dedicated to upper state rotational ("local") quanta (see HITRAN2004 paper [67]).

We also note that in their OFCEAS study of the $\nu_2+\nu_3$ band, Fleurbaey et al. [66] reported the measurement of weaker electric quadrupole lines of the same $\nu_2+\nu_3$ band, together with the detection of the magnetic dipole lines. This detection was made possible by accurate *ab initio* predictions of the E2 line intensities $^{12}C^{16}O_2$ in the 0–10,000 cm$^{-1}$ range [68]. Overall, the *ab initio* intensities of the very weak quadrupole lines are validated by these OFCEAS values (maximum line intensities on the order of $10^{-28}$ cm/molecule). There is also evidence for these quadrupole lines in the ACS Mars spectrum [68]. The weak electric quadrupole lines are not included in the present version of the HITRAN database and will be considered for forthcoming editions.

## 7. The line-shape parameters for the HITRAN2020 $CO_2$ line list

A major update of the line-shape parameters of $CO_2$ broadened by air and $CO_2$ is described in Ref. [13]; this involved both enhancing the HITRAN database and improving completeness. A systematic extrapolation method was introduced for producing the air- and self-broadened half-width Voigt profile parameters for unmeasured transitions [69], based on the measurements reported in Ref. [70]. The temperature-dependent exponents of the air- and self-broadening parameters were generated based on existing measurements and a semi-empirical calculation method using the measurements given in Refs [71,72]. Air- and self-pressure shifts for every line of $CO_2$ were calculated using the semi-empirical approach proposed by Hartmann [73] and fits using carefully selected experimental data.

Besides providing the standard 160-character ".par" parameter, the HITRAN2020 database will include additional parameters for the speed-dependent Voigt (SDV) profile [74,75] in a separate set. The list of the SDV parameters was provided in Table 1 of Ref. [13]. The air- and self-speed dependence of the broadening parameters with their temperature dependence will be added for all the lines of $CO_2$, and they can be downloaded using customized output format on www.hitran.org. One can also retrieve these parameters with the HITRAN application programming interface (HAPI) [76] using the SDVoigt parameters group.

The $CO_2$ line-mixing package, developed by Lamouroux et al. [77], was updated using the new spectroscopic parameters obtained in the present study and the parameters found in Ref. [13]. This package is available at HITRAN*online* and can be used to calculate the $CO_2$ absorption coefficient accounting for the full line-mixing and the first-order line-mixing parameters. Furthermore, as part of the HITRAN2020 extension, the first-order line-mixing parameters were provided for every allowed transition of $CO_2$, and they can be accessed using a user-defined format in HITRAN*online*. The new data were verified using different sets of laboratory spectra to compare with the absorption coefficient calculated by the line-mixing package program. A considerable improvement was achieved for the regions examined compared to HITRAN2016 (we refer to Figs 16-19 in Ref. [13]), which should be beneficial for the $CO_2$ retrieval missions such as the OCO-2, ACE, and GOSAT.

## 8. Overview summary of the HITRAN2020 $CO_2$ line list

The HITRAN2020 line list for the twelve stable isotopic species of carbon dioxide contains 545,084 transitions. It covers the spectral range from 0.757 cm$^{-1}$ to 19,908.186 cm$^{-1}$ with $J \leq 128$ and with the lower-state energies up to 6533.030 cm$^{-1}$. Most of the line positions and their corresponding lower state energies were replaced by using the CDSD-296 database [17]. For the problematic line intensities identified in new laboratory and atmospheric spectra, critical validation tests were performed to improve the accuracy of the $CO_2$ lists. The line-shape parameters of $CO_2$ broadened by air and $CO_2$ were updated. A summary of the $CO_2$ line list in the HITRAN2020 edition compared to the HITRAN2016 is given in Table 2. The HITRAN2020 carbon dioxide line list generated in HITRAN format is available on the HITRAN*online* website

**Table 2**
Comparison of HITRAN2020 and HITRAN2016 line lists for the 12 stable $CO_2$ isotopologues.

| Formula | AFGL code | Abundance | HITRAN2016 | | | HITRAN2020 | | |
|---|---|---|---|---|---|---|---|---|
| | | | Number of lines | Spectral region ($cm^{-1}$) | Q(296 K) | Number of lines | Spectral region ($cm^{-1}$) | Q(296 K) |
| $^{12}C^{16}O_2$ | 626 | 0.984204 | 173,024 | 158.302–14,075.298 | 286.094 | 174,446 | 158.302–19,908.186 | 286.094 |
| $^{13}C^{16}O_2$ | 636 | 0.011057 | 70,577 | 332.649–13,734.963 | 576.644 | 69,870 | 332.649–13,734.963 | 576.644 |
| $^{16}O^{12}C^{18}O$ | 628 | 0.003947 | 127,850 | 1.473–12,677.181 | 607.713 | 122,140 | 1.473–12,677.182 | 607.713 |
| $^{16}O^{12}C^{17}O$ | 627 | $7.339890 \times 10^{-4}$ | 77,941 | 0.757–12,726.562 | 3542.610 | 73,942 | 0.757–12,726.562 | 3542.610 |
| $^{16}O^{13}C^{18}O$ | 638 | $4.434460 \times 10^{-5}$ | 43,782 | 2.945–9212.609 | 1225.270 | 41,058 | 2.945–9212.608 | 1225.270 |
| $^{16}O^{13}C^{17}O$ | 637 | $8.246230 \times 10^{-6}$ | 25,175 | 9.086–8061.741 | 7140.024 | 23,607 | 9.086–8061.739 | 7140.024 |
| $^{12}C^{18}O_2$ | 828 | $3.957340 \times 10^{-6}$ | 10,522 | 482.813–8162.743 | 323.424 | 10,498 | 482.814–8162.752 | 323.424 |
| $^{17}O^{12}C^{18}O$ | 728 | $1.471800 \times 10^{-6}$ | 15,878 | 491.181–8193.172 | 3766.044 | 14,623 | 498.617–8193.172 | 3766.044 |
| $^{12}C^{17}O_2$ | 727 | $1.368470 \times 10^{-7}$ | 6518 | 535.384–6932.693 | 10,971.91 | 6493 | 535.384–6932.693 | 10,971.91 |
| $^{13}C^{18}O_2$ | 838 | $4.446000 \times 10^{-8}$ | 2916 | 539.626–6686.983 | 652.242 | 2926 | 539.620–6686.983 | 652.242 |
| $^{18}O^{13}C^{17}O$ | 837 | $1.653540 \times 10^{-8}$ | 4190 | 549.473–4914.496 | 7593.900 | 3980 | 549.473–4914.496 | 7593.900 |
| $^{13}C^{17}O_2$ | 737 | $1.537500 \times 10^{-9}$ | 1501 | 575.853–3614.084 | 22,129.96 | 1501 | 575.853–3614.084 | 22,129.96 |
| Total | | | 559,874 | | | 545,084 | | |

**Note:** AFGL code is the shorthand notation for the isotopologue, abundance is the terrestrial value assumed by HITRAN, and *Q*(296 K) is the partition sum at the reference temperature of 296 K.

www.hitran.org and Supplementary Material I of this paper. We also present the supplementary "difference" file (Supplementary Material II) that shows every parameter change for each transition between HITRAN2016 and HITRAN2020. This will provide comprehensive information on the changes made in this work, although it will not show the new bands. An overview of the line lists in HITRAN2020 and HITRAN2016 is plotted in Fig. 17**.**

Also, it should be noted that the new version of the Total Internal Partition Sum (TIPS) software was reported for 57 molecules, including $CO_2$, in Ref. [78]. These data are provided with HITRAN2020 and a new version of the TIPS code is available in both FORTRAN and python languages.

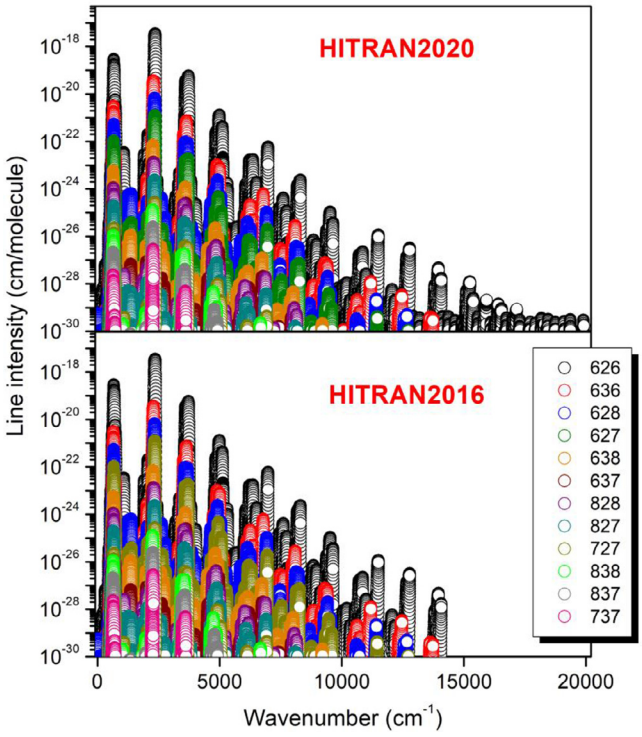


**Fig. 17.** An overview of the HITRAN2016 and HITRAN2020 line lists for the 12 stable $CO_2$ isotopologues: $^{12}C^{16}O_2$ (626), $^{13}C^{16}O_2$ (636), $^{16}O^{12}C^{18}O$ (628), $^{16}O^{12}C^{17}O$ (627), $^{16}O^{13}C^{18}O$ (638), $^{16}O^{13}C^{17}O$ (637), $^{12}C^{18}O_2$ (828), $^{18}O^{12}C^{17}O$ (827), $^{12}C^{17}O_2$ (727), $^{13}C^{18}O_2$ (838), $^{18}O^{13}C^{17}O$ (837), and $^{13}C^{17}O_2$ (737) (The numbers in parentheses are the AFGL shorthand code for the isotopologues).

## 9. Conclusion

This work presents an improved and extended version of the HITRAN2020 spectroscopic database for the carbon dioxide molecule. The database includes updates of the line positions and intensities described in this work, and line shape parameters (described in Hashemi et al. [13]) for 12 stable $CO_2$ isotopologues. Critical validation tests for the spectroscopic data, including the comparisons with the most advanced theoretical and semi-empirical databases [17,18,23,27] and accurate experimental measurements, were carried out. Evaluation of the HITRAN $CO_2$ line lists by comparison to laboratory and atmospheric spectra below 8310 $cm^{-1}$ and the description of the updates made for the bands having mixed CDSD and UCL-IAO line intensities in the HITRAN2016 line list below 8000 $cm^{-1}$ are presented. Recent experimental measurements with sub-percent uncertainty [19–22] were used to improve the $CO_2$ bands in the 1.4- to 2.1-μm region. Several new $CO_2$ bands (more than 3600 transitions) above 8000 $cm^{-1}$ were added to the HITRAN2020 edition from the new high-temperature UCL-4000 $^{12}C^{16}O_2$ line list from the ExoMol [18] database. Also, the updated $CO_2$ line list has been extended by including new experimentally observed bands [14] corresponding to the $^{16}O^{12}C^{18}O$ isotopologue. The magnetic dipole 01111–00001 band of the $^{12}C^{16}O_2$ isotopologue in the 3.3-μm region was introduced into HITRAN for the first time. Updated self- and air-broadened line shape parameters of $CO_2$, as described in Ref. [13] and involved in the enhancement of the HITRAN databases, were also revised. These updates of the $CO_2$ line parameters in HITRAN2020 are expected to have an important impact on the capabilities of current and future remote-sensing missions. The updated line lists for 12 $CO_2$ isotopologues are available as Supplementary material of this paper or can be downloaded from the HITRAN website (www.hitran.org).

## Declaration of Competing Interest

None.

## CRediT authorship contribution statement

**E.V. Karlovets:** Formal analysis, Methodology, Software, Writing – original draft. **I.E. Gordon:** Supervision, Conceptualization, Methodology, Writing – review & editing. **L.S. Rothman:** Writing – review & editing. **R. Hashemi:** Data curation, Writing – review & editing. **R.J. Hargreaves:** Software. **G.C. Toon:** Data curation, Software. **A. Campargue:** Data curation, Writing – review & editing. **V.I.**

**Perevalov:** Data curation, Writing – review & editing. **P. Čermák:** Software. **M. Birk:** Data curation. **G. Wagner:** Data curation. **J.T. Hodges:** Data curation, Writing – review & editing. **J. Tennyson:** Writing – review & editing. **S.N. Yurchenko:** Data curation, Writing – review & editing.

## Acknowledgments

This work was supported by NASA grant funding from AURA NNX17AI78G. The National Institute of Standards and Technology (NIST) received support from the NASA Science Team for the OCO Missions (NRA) NNH17ZDA001N-OCO2 and the NIST Greenhouse Gas and Climate Science Measurements Program. This work was also supported by the Ministry of Science and Higher Education of the Russian Federation. The work performed at UCL was supported by the STFC Projects No. ST/M001334/1 and ST/R000476/1. Part of this work was performed at the Jet Propulsion Laboratory, California Institute of Technology, under contract with NASA. Certain commercial equipment, instruments, or materials are identified in this paper in order to adequately specify the experimental procedure. Such identification is not intended to imply recommendation or endorsement by NIST, nor is it intended to imply that the materials or equipment identified are necessarily the best available for the purpose.

## Supplementary materials

Supplementary material associated with this article can be found, in the online version, at doi:10.1016/j.jqsrt.2021.107896.

## References

[1] Butz A, Guerlet S, Hasekamp O, Schepers D, Galli A, Aben I, et al. Toward accurate $CO_2$ and $CH_4$ observations from GOSAT. Geophys Res Lett 2011;38:2–7. doi:10.1029/2011GL047888.

[2] Alexe M, Bergamaschi P, Segers A, Detmers R, Butz A, Hasekamp O, et al. Inverse modelling of $CH_4$ emissions for 2010-2011 using different satellite retrieval products from GOSAT and SCIAMACHY. Atmos Chem Phys 2015;15:113–33. doi:10.5194/acp-15-113-2015.

[3] Yokota T, Yoshida Y, Eguchi N, Ota Y, Tanaka T, Watanabe H, et al. Global Concentrations of $CO_2$ and $CH_4$ Retrieved from GOSAT : first Preliminary Results. Scientific Online Letters on the Atmosphere 2009;5:160–3. doi:10.2151/sola.2009.041.

[4] Nakajima M, Suto H, Yotsumoto K, Abe M, Kuze A, Shiomi K, et al. Overview of the GOSAT-2 Mission. In: Proceedings of the 29th ISTS; 2013. p. 60.

[5] Oyafuso Fabiano, HPayne Vivienne, JDrouin Brian, Malathy Devi V, Chris Benner D. High accuracy absorption coefficients for the Orbiting Carbon Observatory-2 (OCO-2) mission: validation of updated carbon dioxide cross-sections using atmospheric spectra. J Quant Spectrosc Radiat Transfer 2017;203:213–23. doi:10.1016/j.jqsrt.2017.06.012.

[6] Eldering A, Wennberg PO, Crisp D, Schimel DS, Gunson MR, Chatterjee A, et al. The Orbiting Carbon Observatory-2 early science investigations of regional carbon dioxide fluxes. Science 2017;358:188. doi:10.1126/science.aam5745.

[7] Eldering A, Taylor TE, O'Dell CW, Pavlick R. The OCO-3 mission: measurement objectives and expected performance based on 1 year of simulated data. Atmos Meas Tech 2019;12:2341–70. doi:10.5194/amt-12-2341-2019.

[8] Fischer H, Birk M, Blom C, Carli B, Carlotti M, von Clarmann T, et al. MIPAS: an instrument for atmospheric and climate research. Atmos Chem Phys 2008;8:2151–88. doi:10.5194/acp-8-2151-2008.

[9] Bernath PF, McElroy CT, Abrams MC, Boone CD, Butler M, Camy-Peyret C, et al. Atmospheric chemistry experiment (ACE): mission overview. Geophys Res Lett 2005;32:1–5. doi:10.1029/2005GL022386.

[10] Wunch D, Toon GC, Blavier JFL, Washenfelder RA, Notholt J, Connor BJ, et al. The total carbon column observing network. Philos Trans R Soc, A 2011;369:2087–112. doi:10.1098/rsta.2010.0240.

[11] Hase F. Improved instrumental line shape monitoring for the ground-based, high-resolution FTIR spectrometers of the Network for the Detection of Atmospheric Composition Change. Atmos Meas Tech 2012;5:603–10. doi:10.5194/amt-5-603-2012.

[12] Gordon IE, Rothman LS, Hill C, Kochanov RV, Tan Y, Bernath PF, et al. The HITRAN2016 molecular spectroscopic database. J Quant Spectrosc Radiat Transfer 2017;203:3–69. doi:10.1016/j.jqsrt.2017.06.038.

[13] Hashemi R, Gordon IE, Tran H, Kochanov RV, Karlovets EV, Tan Y, Lamouroux J, et al. Revising the line-shape parameters for air- and self- broadened $CO_2$ lines toward a sub-percent accuracy level. JQSRT 2020;256:107283. doi:10.1016/j.jqsrt.2020.107283.

[14] Karlovets EV, Kassi S, Campargue A. Journal of Quantitative Spectroscopy & Radiative Transfer High sensitivity CRDS of $CO_2$ in the 1.18 $\mu$m transparency window. Validation tests of current spectroscopic. databases 2020;247:1–8. https://doi.org/10.1016/j.jqsrt.2020.106942.

[15] Toon GC. $CO_2$ Spectroscopy Evaluation: 670 to 8310 $cm^{-1}$, Reports and Presentations for the HITRAN meeting, Jun 2020. Jet Propulsion Laboratory, California Institute of Technology; 2020. https://mark4sun.jpl.nasa.gov/report/CO2_Spectroscopy_Evaluation_20190503-compressed.pdf.

[16] Toon GC. $CO_2$ Spectroscopy Evaluation: 670 to 7000 $cm^{-1}$, Reports and Presentations for the ACE STM, Oct 2018. Jet Propulsion Laboratory, California Institute of Technology; 2018. https://mark4sun.jpl.nasa.gov/report/CO2_Spectroscopy_Evaluation_highlights-compressed.pdf.

[17] Tashkun SA, Perevalov VI, Gamache RR, Lamouroux J. CDSD-296, high-resolution carbon dioxide spectroscopic databank: an update. J Quant Spectrosc Radiat Transfer 2019;228:124–31. doi:10.1016/j.jqsrt.2019.03.001.

[18] Yurchenko SN, Mellor TM, Freedman RS, Tennyson J. ExoMol line lists-XXXIX. Ro-vibrational molecular line list for $CO_2$. Mon Not R Astron Soc 2020;496:5282–91. doi:10.1093/mnras/staa1874.

[19] Long DA, Reed ZD, Fleisher AJ, Mendonca J, Roche S, Hodges JT. High-Accuracy Near-Infrared Carbon Dioxide Intensity Measurements to Support Remote Sensing. Geophys Res Lett 2020;47 e2019GL086344. doi:10.1029/2019GL086344.

[20] Fleurbaey H, Yi H, Adkins EM, Fleisher AJ, Hodges JT. Cavity ring-down spectroscopy of $CO_2$ near $\lambda = 2.06$ µm: accurate transition intensities for the Orbiting Carbon Observatory-2 (OCO-2) "strong band. J Quant Spectrosc Radiat Transfer 2020;252:107104. doi:10.1016/j.jqsrt.2020.107104.

[21] Birk M, Röske C, Wagner C. Measurement and line parameter database $CO_2$ 6000-7000 $cm^{-1}$. Zenodo 2021.

[22] Birk M, Röske C, Wagner C. High accuracy $CO_2$ Fourier transform measurements in the range 6000–7000 $cm^{-1}$. J Quant Spectrosc Radiat Transfer 2021;272:107791. doi:10.1016/j.jqsrt.2021.107791.

[23] Huang X, Richard S, Freedman B, Lee TJ. Ames-2016 line lists for 13 isotopologues of $CO_2$: updates, consistency, and remaining issues. J Quant Spectrosc Radiat Transfer 2017;203:224–41. doi:10.1016/j.jinf.2020.02.020.

[24] Gordon IE, Rothman LS, Hargreaves Hashemi R, Karlovets EV, Skinner FM, Conway EK, Hill C, et al. The HITRAN2020 molecular spectroscopic database. J Quant Spectrosc Radiat Transfer 2021 Submitted to HITRAN2020 Special Issue.

[25] Hill C, Gordon IE, Kochanov RV, Barrett L, Wilzewski JS, Rothman LS. HITRANonline: an online interface and the flexible representation of spectroscopic data in the HITRAN database. J Quant Spectrosc Radiat Transfer 2016;177:4–14. doi:10.1016/j.jqsrt.2015.12.012.

[26] Tashkun SA, Perevalov VI, Gamache RR, Lamouroux J. CDSD-296, high resolution carbon dioxide spectroscopic databank: version for atmospheric applications. J Quant Spectrosc Radiat Transfer 2015;152:45–73. doi:10.1016/j.jqsrt.2014.10.017.

[27] Zak E, Tennyson J, Polyansky OL, Lodi L, Zobov NF, Tashkun SA, et al. A room temperature $CO_2$ line list with ab initio computed intensities. J Quant Spectrosc Radiat Transfer 2016;177:31–42. doi:10.1016/j.jqsrt.2015.12.022.

[28] Zak EJ, Tennyson J, Polyansky OL, Lodi L, Zobov NF, Tashkun SA, et al. Room temperature linelists for $CO_2$ asymmetric isotopologues with ab initio computed intensities. J Quant Spectrosc Radiat Transfer 2017;203:265–81. doi:10.1016/j.jqsrt.2017.01.037.

[29] Zak EJ, Tennyson J, Polyansky OL, Lodi L, Zobov NF, Tashkun SA, et al. Room temperature linelists for $CO_2$ symmetric isotopologues with ab initio computed intensities. J Quant Spectrosc Radiat Transfer 2017;189:267–80. doi:10.1016/j.jqsrt.2015.12.022.

[30] Teffo JL, Sulakshina ON, Perevalov VI. Effective Hamiltonian for rovibrational energies and line intensities of carbon dioxide. J Mol Spectrosc 1992;156:48–64. doi:10.1016/0022-2852(92)90092-3.

[31] Teffo JL, Lyulin OM, Perevalov VI, Lobodenko EI. Application of the effective operator approach to the calculation of $^{12}C^{16}O_2$ line intensities. J Mol Spectrosc 1998;187:28–41. doi:10.1006/jmsp.1997.7455.

[32] Polyansky OL, Bielska K, Ghysels M, Lodi L, Zobov NF, Hodges JT, et al. High-Accuracy $CO_2$ Line Intensities Determined from Theory and Experiment. Phys Rev Lett 2015;114:1–5. doi:10.1103/PhysRevLett.114.243001.

[33] Yurchenko SN, Thiel W, Jensen P. Theoretical ROVibrational Energies (TROVE): a robust numerical approach to the calculation of rovibrational energies for polyatomic molecules. J Mol Spectrosc 2007;245:126–40. doi:10.1016/j.jms.2007.07.009.

[34] Benner Chris, Devi VMalathy, Rinsland Curtis P, Ferry-Leeper Penelope S. Absolute intensities of $CO_2$ lines in the 3140–3410-$cm^{-1}$ spectral region. Appl Opt 1988;27:1588–97. doi:10.1364/AO.27.001588.

[35] Toth RA, Brown LR, Miller CE, Devi VM, Benner DC. Spectroscopic database of $CO_2$ line parameters: 4300–7000 $cm^{-1}$. J Quant Spectrosc Radiat Transfer 2008;109:906–21. doi:10.1016/j.jqsrt.2007.12.004.

[36] Tanaka Tomoaki, Fukabori Masashi, Sugita Takafumi, Nakajima Hideaki, et al. Spectral line parameters for $CO_2$ bands in the 4.8- to 5.3-$\mu$m region. J Mol Spectrosc 2006;239:1–10. doi:10.1016/j.jms.2006.05.013.

[37] Rinsland CP, Benner DC, Devi VM. Measurements of absolute line intensities in carbon dioxide bands near 5.2 $\mu$m. Appl Opt 1985;24:1644. doi:10.1364/ao.24.001644.

[38] Karlovets EV, Kassi S, Tashkun SA, Perevalov VI, Campargue A. High sensitivity Cavity Ring Down spectroscopy of carbon dioxide in the 1.19-1.26 $\mu$m region. J Quant Spectrosc Radiat Transfer 2014;144:137–53. doi:10.1016/j.jqsrt.2014.04.001.

[39] Čermák P, Karlovets EV, Mondelain D, Kassi S, Perevalov VI, Campargue A. High sensitivity CRDS of $CO_2$ in the 1.74 µm transparency window. A validation test for the spectroscopic databases. J Quant Spectrosc Radiat Transfer 2018;207:95–103. doi:10.1016/j.jqsrt.2017.12.018.
[40] Karlovets EV, Čermák P, Mondelain D, Kassi S, Campargue A, Tashkun SA, et al. Analysis and theoretical modeling of the $^{18}O$ enriched carbon dioxide spectrum by CRDS near 1.74 µm. J Quant Spectrosc Radiat Transfer 2018;217:73–85. doi:10.1016/j.jqsrt.2018.05.017.
[41] Rinsland CP, Benner DC. Absolute intensities of spectral lines in carbon dioxide bands near 2050 $cm^{-1}$. Appl Opt 1984;23:4523–8. doi:10.1364/AO.23.004523.
[42] Rinsland CP, Benner DC, VM Devi. Absolute line intensities in $CO_2$ bands near 4.8 $\mu$m. Appl Opt 1986;25:1204–14. doi:10.1364/AO.25.001204.
[43] Rothman LS, Gordon IE, Barbe A, Benner DC, Bernath PF, Birk M, et al. The HITRAN2008 molecular spectroscopic database. J Quant Spectrosc Radiat Transfer 2009;110:533–72. doi:10.1016/j.jqsrt.2009.02.013.
[44] Rothman LS, Gordon IE, Babikov Y, Barbe A, Chris Benner D, Bernath PF, et al. The HITRAN2012 molecular spectroscopic database. J Quant Spectrosc Radiat Transfer 2013;130:4–50. doi:10.1016/j.jqsrt.2013.07.002.
[45] Wunch D, Toon GC, Blavier JFL, Washenfelder RA, Notholt J, Connor BJ, et al. GFIT. Philosophical Transactions of the Royal Society A: mathematical. Physical and Engineering Sciences 2011;369:2087–112. doi:10.1098/rsta.2010.0240.
[46] Karlovets EV, Sidorenko AD, Mondelain D, Kassi S, Campargue A, Sidorenko AD, et al. The $^{13}CO_2$ absorption spectrum by CRDS near 1.74 µm. J Mol Spectrosc 2018;354:54–9. doi:10.1016/j.jms.2018.10.003.
[47] Giver Lawrence, Brown Linda, Chackerian Charles, Freedman Richard. The rovibrational intensities of five absorption bands of $^{12}C^{16}O_2$ between 5218 and 5349 $cm^{-1}$. J Quant Spectrosc Radiat Transfer 2003;78(3–4):417–36 417–36. doi:10.1016/S0022-4073(02)00277-7.
[48] Perevalov BV, Kassi S, Romanini D, Perevalov VI, Tashkun SA, Campargue A. CW-cavity ringdown spectroscopy of carbon dioxide isotopologues near 1.5 $\mu$m. J Mol Spectrosc 2006;238:241–55. doi:10.1016/j.jms.2006.05.009.
[49] Miller CE, Crisp D, DeCola PL, Olsen SC, Randerson JT, Michalak AM, et al. Precision requirements for space-based $XCO_2$ data. J. Geophys. Res. Atmosph. 2007;112:1–19. doi:10.1029/2006JD007659.
[50] Campbell JF, Lin B, Dobler J, Pal S, Davis K, Erxleben W, McGregor D, O'Dell C, Bell E, et al. Field Evaluation of Column $CO_2$ Retrievals From Intensity-Modulated Continuous-Wave Differential Absorption Lidar Measurements During the ACT-America Campaign. Earth and Space Sci. 2020;7 e2019EA000847. doi:10.1029/2019EA000847.
[51] Guo R, Teng J, Dong H, Zhang T, Li D, Wang D. Line parameters of the P-branch of (30012) ← (00001) $^{12}C^{16}O_2$ band measured by comb-assisted, Pound-Drever-Hall locked cavity ring-down spectrometer. J Quant Spectrosc Radiat Transfer 2021;264:107555. doi:10.1016/j.jqsrt.2021.107555.
[52] Wu H, Hu C-L, Wang J, Sun Yu R, Tan Y, et al. A Well-Isolated Vibrational State of $CO_2$ Verified by near-infrared saturated spectroscopy with kHz accuracy". Phys Chem Chem Phys 2020;22:2841–8. doi:10.1039/C9CP05121J.
[53] Truong GW, Long DA, Cygan A, Lisak D, et al. Comb-linked, cavity ring-down spectroscopy for measurements of molecular transition frequencies at the kHz-level. J Chem Phys 2013;138(9):094201. doi:10.1063/1.4792372.
[54] Gatti D, Sala T, Gotti R, Cocola L, Poletto L, Prevedelli M, et al. Comb-locked cavity ring-down spectrometer. J Chem Phys 2015;142(7):074201. doi:10.1063/1.4907939.
[55] Long DA, Wójtewicz S, Miller CE, Hodges JT. Frequency-agile, rapid scanning cavity ring-down spectroscopy (FARS-CRDS) measurements of the (30012) ← (00001) near-infrared carbon dioxide band. J Quant Spectrosc Radiat Transfer 2015;161:35–40. doi:10.1016/j.jqsrt.2015.03.031.
[56] Guo R, Teng J, Cao K, Dong H, Cui W, Zhang T. Comb-assisted, Pound-Drever-Hall locked cavity ring-down spectrometer for high-performance retrieval of transition parameters. Opt Express 2019;27:31850–63. doi:10.1364/OE.27.031850.
[57] Long DA, Truong G-W, Hodges JT, Miller CE. Absolute $^{12}C^{16}O_2$ transition frequencies at the kHz-level from 1.6 to 7.8 µm. J Quant Spectrosc Radiat Transfer 2013;130:112–15. doi:10.1016/j.jqsrt.2013.07.001.
[58] Burkart J, Sala T, Romanini D, Marangoni M, Campargue A, Kassi S. Saturated $CO_2$ absorption near 1.6 $\mu$m for kilohertz accuracy transition frequencies. J Chem Phys 2015;142:191103. doi:10.1063/1.4921557.
[59] Tennyson J, Yurchenko SN, Al-Refaie AF, Clark VHJ, Chubb KL, Conway EK, Dewan A, Gorman MN, Hill C, et al. The 2020 release of the ExoMol database: molecular line lists for exoplanet and other hot atmospheres. J Quant Spectrosc Radiat Transfer 2020;255:107228. doi:10.1016/j.jqsrt.2020.107228.
[60] Rothman LS, Hawkins RL, Wattson RB, Gamache RR. Energy levels, intensities, and linewidths of atmospheric carbon dioxide bands. J Quant Spectrosc Radiat Transfer 1992;48:537–66. doi:10.1016/0022-4073(92)90119-O.
[61] Trokhimovskiy A, Perevalov V, Korablev O, Fedorova A, Olsen KS, Bertaux JL, et al. First observation of the magnetic dipole $CO_2$ main isotopologue absorption band at 3.3 µm in the atmosphere of Mars by the ExoMars Trace Gas Orbiter ACS instrument. Astronomy & Astrophysics 2020;639:1–7. doi:10.1051/0004-6361/202038134.
[62] Korablev O, Montmessin F, Trokhimovskiy A, Fedorova AA, Shakun AV, Grigoriev AV, et al. The Atmospheric Chemistry Suite (ACS) of Three Spectrometers for the ExoMars 2016 Trace Gas Orbiter. Space Sci Rev 2018;214:7. doi:10.1007/s11214-017-0437-6.
[63] Perevalov VI, Trokhimovskiy AY, Lukashevskaya AA, Korablev OI, et al. Magnetic dipole and electric quadrupole absorption in carbon dioxide. J Quant Spectrosc Radiat Transfer 2021;259:107408. doi:10.1016/j.jqsrt.2020.107408.
[64] Borkov YG, Solodov AM, Solodov AA, Perevalov VI. Line intensities of the 01111–00001 magnetic dipole absorption band of $^{12}C^{16}O_2$: laboratory measurements. J Mol Spectrosc 2021;376:111418. doi:10.1016/j.jms.2021.111418.
[65] Majcherova Z, MacKo P, Romanini D, Perevalov VI, Tashkun SA, Teffo JL, et al. High-sensitivity CW-cavity ringdown spectroscopy of $^{12}CO_2$ near 1.5 $\mu$m. J Mol Spectrosc 2005;230:1–21. doi:10.1016/j.jms.2004.09.011.
[66] Fleurbaey H, Grilli R, Mondelain D, Kassi S, Yachmenev A, Yurchenko SN, Campargue A. Electric-quadrupole and magnetic-dipole conitributions to the $\nu_2+\nu_3$ band of carbon dioxide near 3.3 µm. J Quant Spectrosc Radiat Transfer 2021;266:107558. doi:10.1016/j.jqsrt.2021.107558.
[67] Rothman LS, Jacquemart D, Barbe A, Benner DC, Birk M, Brown LR, et al. The HITRAN 2004 molecular spectroscopic database. J Quant Spectrosc Radiat Transfer 2005;96:139–204. doi:10.1016/j.jqsrt.2004.10.008.
[68] Yachmenev A, Küpper J, Campargue A, Yurchenko SN, Küpper J, Tennyson J. Electric quadrupole transitions in carbon dioxide. J Chem Physics 2021;154:211104 (in press). doi:10.1063/5.0053279.
[69] Voigt W. Über das Gesetz Intensitätsverteilung innerhalb der Linien eines Gasspektrums. München; Berlin: sitzber. Bayr Akad 1912:603.
[70] Hashemi R, Rozario H, Ibrahim A, Predoi-Cross A. Line shape study of the carbon dioxide laser band. Can J Phys 2013;91(11):924–36. doi:10.1139/cjp- 2013- 0051.
[71] Ma H, Sun M, Zha S, Liu Q, Cao Z, Huang Y, et al. Temperature dependence of line parameters of $CO_2$ near 2.004 $\mu$m studied by tunable diode laser spectroscopy. Chin Phys B 2018;27(2):023301. doi:10.1088/1674-1056/27/2/023301.
[72] Predoi-Cross A, Liu W, Murphy R, Povey C, Gamache R, Laraia A, et al. Measurement and computations for temperature dependences of self-broadened carbon dioxide transitions in the 30012-00001 and 30013-00001 bands. J Quant Spectrosc Radiat Transfer 2010;111(9):1065–79. doi:10.1016/j.jqsrt.2010.01.003.
[73] Hartmann J-M. A simple empirical model for the collisional spectral shift of air-broadened $CO_2$ lines. J Quant Spectrosc Radiat Transfer 2009;110(18):2019–26. doi:10.1016/j.jqsrt.2009.05.016.
[74] Pickett HM. Effects of velocity averaging on the shapes of absorption lines. J Chem Phys 1980;73(12):6090–4. doi:10.1063/1.440145.
[75] Pine AS. Line shape asymmetries in Ar-broadened HF ($v = 10$) in the Dicke arrowing regime. J Chem Phys 1994;101(5):3444–52. doi:10.1063/1.467529.
[76] Kochanov RV, Gordon IE, Rothman LS, Wcisło P, Hill C, Wilzewski JS. HITRAN Application Programming Interface (HAPI): a comprehensive approach to working with spectroscopic data. J Quant Spectrosc Radiat Transfer 2016;177:15–30. doi:10.1016/j.jqsrt.2016.03.005.
[77] Lamouroux J, Régalia L, Thomas X, Auwera JV, Gamache RR, Rothman LS, Gordon IE, Hartmann J-M. $CO_2$ Line-mixing database and software update and its tests in the 2.1 $\mu$m and 4.3 $\mu$m regions. J Quant Spectrosc Radiat Transfer 2015;151:88–96. doi:10.1016/j.jqsrt.2014.09.017.
[78] Gamache RR, Vispoel B, Rey M, Nikitin A, Tyuterev V, Egorov O, Gordon IE, Boudon V. Total internal partition sums for the HITRAN2020 database. J Quant Spectrosc Radiat Transfer 2021;271:107713. doi:10.1016/j.jqsrt.2021.107713.